2.3. Exosome isolation and purification

Mo-DCs were generated from PBMCs with GM-CSF and IL-4 as described above. Seven days after the initiation of culture, Mo-DC culture supernatants were collected. Exosomes were isolated as previously described but with minor modifications [11,12]. Culture supernatants were centrifuged at 300g for 5 min and then at 1200g for 20 min to eliminate cells and debris. Cell-free supernatants were clarified through a 0.2-μm filter (Sartorius AG, Goettingen, Germany) to reduce the number of contaminating large vesicles shed from the plasma membrane. The clarified supernatant was subsequently concentrated through a 100-kDa membrane (YM-100, Microcon, Millipore, Billerica, MA, USA). In some experiments, this concentration procedure was repeated five times with PBS (Wako Pure Chemical Industries, Osaka, Japan) to eliminate the original culture supernatant. The concentrated materials were resuspended in RPMI medium at the original volume of the supernatant. This preparation was denoted crude exosomes.

Exosomes were further purified with human anti-HLA-DP, -DQ, or -DR-coated paramagnetic beads (average size: 4.5 μm, Dynal). Briefly, human anti-HLA-DP, -DQ, or -DR-coated paramagnetic beads were washed with PBS. And 1.0×10^6 DC-derived exosomes were mixed with 1.0×10^6 paramagnetic beads. The mixture was incubated at 4 °C for 24 h on a rotating plate, and the beads were washed twice on a magnetic rack with PBS containing 3% BSA (Sigma) and 0.1% NaN_3 (Sigma) (referred to as FACS buffer) to eliminate unbound or excess exosomes. Finally, exosomes coupled to the beads were resuspended in RPMI medium at the original volume of the exosome-containing medium. This preparation was denoted purified exosomes.

2.4. Naive CD4$^+$ T cell culture

CD4$^+$ T cells were suspended at a cell density of 1.0×10^6/ml, and 1.5×10^5 CD4$^+$ T cells were plated in a 96-well flat-bottomed culture plate (150 μl) and cultured at 37 °C for the indicated times. In an experiment using separated cell-culture system, CD4$^+$ T cells (1.5×10^6 cells) were cultured with Mo-DCs (1.5×10^5 cells) in 1.5 ml of RPMI medium or were cultured separately in RPMI medium (1.5 ml) with a 0.4-μm separated cell-culture system (Becton–Dickinson). Cellular viability and the number of CD4$^+$ T cells were determined by trypan blue dye exclusion and a cell counter (CDA-500, Sysmex Mundelin, IL, USA), respectively. T cells and DCs were easily distinguishable with each cell size using a cell counter.

2.5. Blocking assay for MHC class II molecules

To examine the effect of MHC class II proteins on Mo-DCs or of exosome preparations on naive CD4$^+$ T cell survival, Mo-DCs (1.0×10^5 cells/ml), crude exosomes, or purified exosomes prepared from 1×10^5 Mo-DC/ml were preincubated with anti-MHC class II mAb (4 μg/ml, Diaclone Research Besaucon, France) at 37 °C for 1 h, and CD4$^+$ T cells (1.0×10^6 cells/ml) were added and cultured at 37 °C for 4 days. Isotype-matched IgG1 mAb was used as a control.

2.6. FACS analysis

A 10× concentrate of crude exosomes (100 μl) was mixed with 100 μl FITC-conjugated anti-HLA-DR mAb and PE-conjugated anti-CD86 mAb. After a 30-min incubation at 4 °C, the samples were diluted with FACS buffer, and the fluorescence intensities of the exosome preparations were measured with a FACS Calibur flow cytometer and were analyzed with CELLQuest software.

Purified exosomes were prepared with human anti-HLA-DP, -DQ, or -DR-coated paramagnetic beads as described above. Purified exosomes (10 μl) were suspended in 100 μl FACS buffer, mixed with FITC-conjugated anti-HLA-DR mAb (10 μl) and PE-conjugated anti-CD86 mAb (10 μl), and incubated at 4 °C for 30 min. The samples were washed twice on a magnetic rack with FACS buffer, followed by reconstitution of the bead pellets in buffer containing 1% formaldehyde. Stained and fixed exosome-coupled beads were analyzed on a FACS Calibur flow cytometer with CELLQuest software.

2.7. Electrophoretic mobility shift assay

NF-κB activity in nuclei isolated from naive CD4$^+$ T cells was determined by electrophoretic mobility shift assay (EMSA). Extraction of nuclear proteins and EMSA were performed as described previously [27]. Briefly, 5 μg of nuclear protein was incubated for 30 min at room temperature with binding buffer (20 mM Hepes–NaOH, pH 7.9, 2 mM EDTA, 100 mM NaCl, 10% glycerol, and 0.2% NP-40), poly(dI–dC), and ^{32}P-labeled double-stranded oligonucleotide containing the NF-κB binding motif (Promega, Madison, WI, USA). The sequence of the double-stranded oligomer used for EMSA is as follows: 5'-AGTTGAGGGGACTTTCCC AGGC-3' (sense strand). The reaction mixtures were loaded on a 4% polyacrylamide gel and electrophoresed with running buffer 0.25× TBE. After the gel was dried, DNA–protein complexes were visualized by autoradiography.

2.8. Electron microscopy

Exosome-bead complexes were fixed in 3% glutaraldehyde in 0.1 M cacodylate buffer (CB) at pH 7.3 for 3 h at 4 °C and washed in 0.1 M CB. The complexes were resuspended and embedded in 4% agar [28]. After the

agar was cut into 1-mm³ pieces, the pieces were fixed in 1% osmium tetroxide in 0.1 M CB overnight and washed in distilled water. The specimens were dehydrated in a graded series of ethanol and embedded in Epon 812. Ultrathin sections were treated with uranyl acetate followed by lead citrate and were examined with an electron microscope (JEM-1200EX, JEOL, Tokyo, Japan).

2.9. Statistical analysis

Comparison of means among three or more groups was done by the Scheffé's method. All results with a p value of less than 0.05 were considered statistically significant.

3. Results

3.1. Mo-DCs support naive CD4⁺ T cell survival

When naive CD4⁺ T cells were cultured in RPMI medium in the absence of Mo-DCs, CD4⁺ T cell numbers decreased daily. Coculture of CD4⁺ T cells with Mo-DCs at a ratio of 10:1 significantly supported CD4⁺ T cell survival (Fig. 1A). Mo-DCs supported CD4⁺ T cell survival in a dose-dependent manner (Fig. 1B). Taken together, CD4⁺ T cells and Mo-DCs were principally used at a cell ratio of 10:1 throughout this study. To examine whether direct contact between CD4⁺ T cells and Mo-DCs was required to support CD4⁺ T cell survival, we used a separated cell-culture system as described in Materials and methods. When CD4⁺ T cells were cultured without direct contact with Mo-DCs, the number of CD4⁺ T cells decreased compared to that in mixed cultures but increased significantly compared to that of CD4⁺ T cells alone (Fig. 2A). Because it is believed that small Mo-DC-derived components that can pass through 0.4-μm filters may have a supportive effect on naive CD4⁺ T cell survival, we speculated that cytokines such as IL-4, IL-7, or IL-15 may be involved. Culture supernatants were filtered with a filter that allows components smaller than 100 kDa to pass through. Both passed (cytokine-rich) and nonpassed (cytokine-poor) fractions were re-adjusted to the original volume with RPMI medium. Contrary to our expectation, the nonpassed fraction but not the passed fraction supported naive CD4⁺ T cell survival (Fig. 2B).

We next examined which molecules contribute to the prolonged in vitro survival of naive CD4⁺ T cells. We focused on MHC class II proteins, particularly HLA-DR, which is expressed on Mo-DCs. Pretreatment of Mo-DCs with anti-HLA-DR mAb inhibited the supportive effect on CD4⁺ T cell survival (Fig. 3A). Interestingly, addition of anti-HLA-DR mAb to the nonpassed fraction also significantly decreased the number of cells (Fig. 3B).
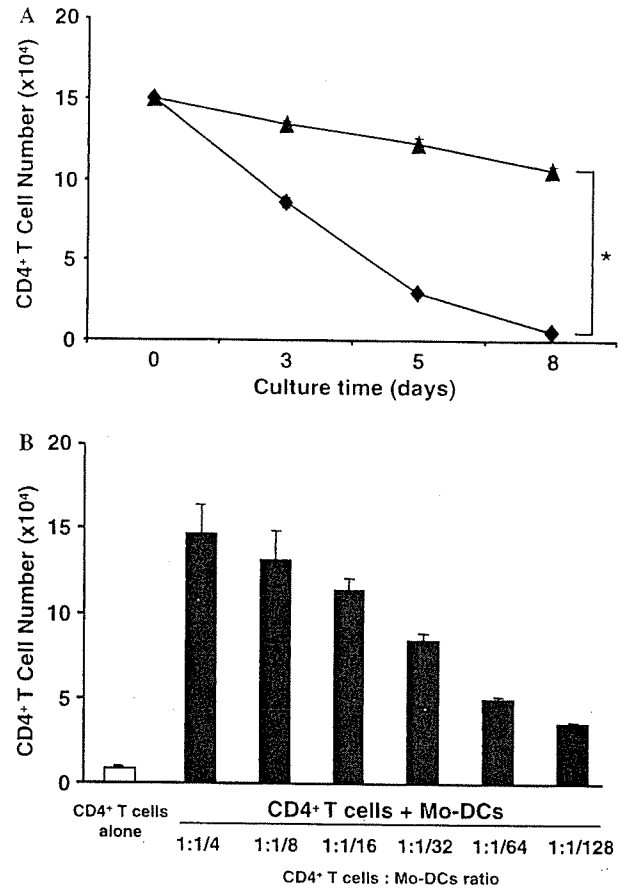

Fig. 1. Coculture with Mo-DCs supports naive CD4⁺ T cell survival. (A) Purified naive CD4⁺ T cells were cultured in RPMI medium with (closed triangle) or without (closed diamond) autologous Mo-DCs at a ratio of 10:1. Cell numbers of the viable CD4⁺ T cells were counted on the indicated days after dead cell exclusion by trypan blue staining. Values represent the means ± SD of triplicate determinations. The asterisk indicates significant differences <0.0001. The data are representative of six independent experiments using Mo-DCs and CD4⁺ T cells obtained from three different healthy donors. (B) Mo-DCs support naive CD4⁺ T cell survival in a dose-dependent manner. Purified naive CD4⁺ T cells (1.5 × 10⁵/150 μl) were cultured with indicated cell numbers of Mo-DCs for 5 days. The data are representative of three independent experiments using Mo-DCs and CD4⁺ T cells obtained from three different healthy donors.

3.2. Exosomes are present in Mo-DC culture supernatant

We speculated that the HLA-DR-bearing components in the nonpassed fraction may be insoluble substances such as membrane fragments or exosomes. Crude exosomes and purified exosomes were collected from Mo-DC culture supernatants as described in Materials and methods. FACS analysis revealed that 21.5% of the particles in the crude exosomes were positive for both HLA-DR and CD86 (data not shown). The FACS cytogram of purified exosomes coupled to mAb-coated beads showed three populations: single beads, clumps of two beads, and clumps of three or more beads, from the dot-plot representation of forward and side scatter (Fig. 4A-1), as described previously [29]. Single beads represented more
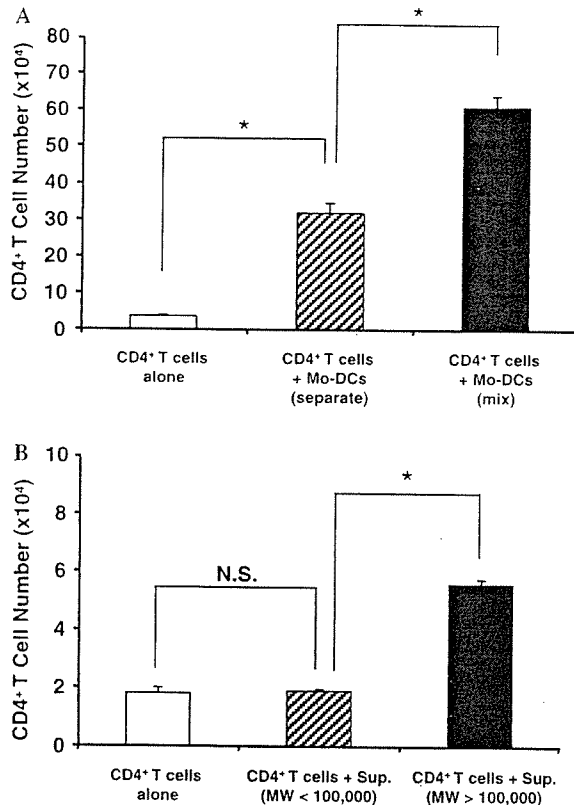
Fig. 2. Supportive effects of Mo-DCs on naive CD4$^+$ T cell survival without direct cellular contact. (A) Viable cell numbers of naive CD4$^+$ T cells cultured in chambers separated by a membrane with pores from Mo-DCs (hatched column) or in the mixture without separation (filled column) were counted on day 5. In only this experiment using separated cell-culture system, CD4$^+$ T cells (1.5 × 10^6 cells) were cultured with Mo-DCs (1.5 × 10^5 cells) in 1.5 ml of RPMI medium or were cultured separately in RPMI medium (1.5 ml) with a 0.4-µm separated cell-culture system. Open column shows the cell number of viable naive CD4$^+$ T cells cultured without Mo-DCs. Values represent means ± SD of triplicate determinations. The asterisks indicate significant differences <0.0001. The data are representative of three independent experiments using Mo-DCs and CD4$^+$ T cells obtained from three different healthy donors. (B) Naive CD4$^+$ T cells were cultured in the presence of the culture supernatant of Mo-DCs for 3 days and then the viable cell numbers of the cells were counted. Each column shows the viable cell numbers of the T cells cultured with components smaller than MW 100,000 (hatched column), those larger than MW 100,000 (closed column) or RPMI medium only (open column). Values represent means ± SD of triplicate determinations. The asterisk indicates significant differences 0.0004. N.S. shows not significant. The data are representative of three independent experiments using Mo-DCs and CD4$^+$ T cells obtained from three different healthy donors.

than 85% of the total number. The populations containing clumped beads were removed from the analysis by gating for single beads only. More than 90% of the single beads were positive for both HLA-DR and CD86 (Fig. 4A-2). These data indicate that 20% of the particles in the crude exosomes and 90% of the particles in the purified exosomes consist of intact HLA-DR- and CD86-expressing exosomes. Electron microscopic analysis confirmed that the substances coupled to the beads were exosomes (Figs. 4B-1 and B-2). These substances showed the
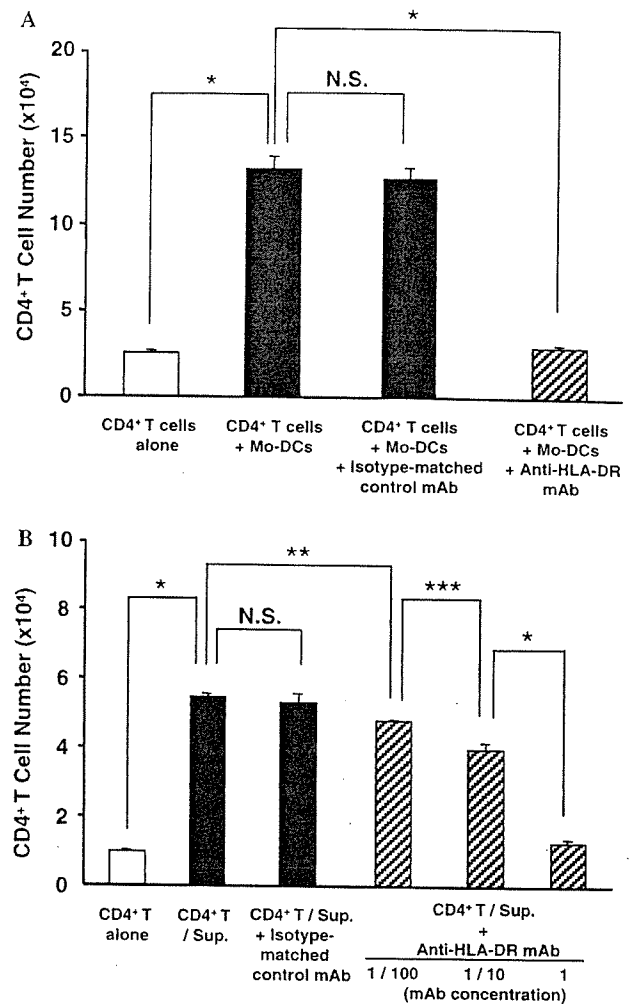

Fig. 3. Requirement of TCR-MHC class II interaction for the prolonged naive CD4$^+$ T cells survival. (A) Viable cell numbers of naive CD4$^+$ T cells cultured with Mo-DCs for 5 days in the presence of anti-MHC class II mAb (4 µg/ml) (hatched column) or isotype-matched control mAb (closed column) were shown. The asterisk indicates significant differences <0.0001. N.S. shows not significant. (B) Naive CD4$^+$ T cells were cultured in the presence of the culture supernatant of Mo-DCs (components of larger than MW 100,000) with anti-MHC class II mAb (hatched column) or with isotype-matched control mAb (closed column) for 4 days and then the viable cell numbers of the cells were counted. The asterisks indicate significant differences <0.0001 (*), 0.002 (**), and 0.007 (***). N.S. shows not significant. Values represent means ± SD of triplicate determinations. The data are representative of three independent experiments using Mo-DCs and CD4$^+$ T cells obtained from three different healthy donors.

characteristic saucer-like morphology of a flattened sphere limited by a lipid bilayer. The exosomes coupled to the beads ranged from 40 to 140 nm in diameter (means ± SD, 78.46 ± 11.04 nm). The average size of a bead and a CD4$^+$ T cell is 4500 and 7250 nm, respectively.

3.3. Mo-DC-derived exosomes support naive CD4$^+$ T cell survival

To confirm that exosomes are involved in supporting in vitro naive CD4$^+$ T cell survival, purified exosomes
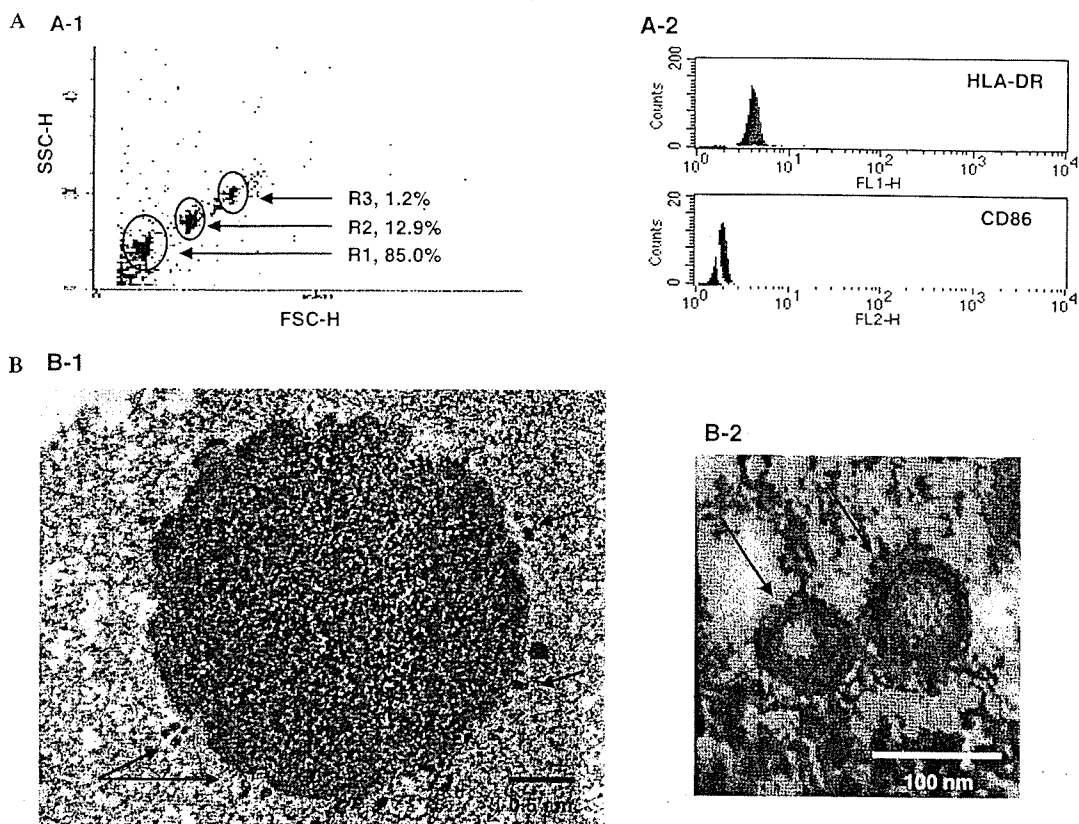
Fig. 4. Detection of MHC class II and CD86 molecules in the components of over MW 100,000 supernatant and electron microscopic characterization of the component. (A) Purified components in supernatants coupled with anti-HLA-DR mAb-coated beads were stained with anti-HLA-DR or anti-CD86 mAbs, and then analyzed by FACS. Three populations of the stained beads appeared in the forward (FSC) and side scatter (SSC) plot are indicated as R1, R2, and R3, respectively and the percentages of each population are also shown (A-1). Histograms show staining of beads for anti-HLA-DR or anti-CD86 (filled line) or control IgG (bold line) on gated R1 area (A-2). The data are representative of three independent experiments. (B) Purified components in supernatants coupled with beads were characterized by electron microscope. Small vesicles (arrows) coating on the surface of the bead (B-1), bar = 0.5 μm and two vesicles of higher magnification (B-2) are shown, bar = 100 nm. The data are representative of six independent experiments using Mo-DCs and CD4$^+$ T cells obtained from three different healthy donors.

coupled to mAb-coated beads were used as effector components. Purified exosomes but not beads alone significantly supported naive CD4$^+$ T cell survival in a dose-dependent manner (Fig. 5A). When beads alone were added to CD4$^+$ T cells, several dying cells were found, and the beads did not bind firmly to any CD4$^+$ T cells. When exosome-coupled beads (purified exosomes) were added to CD4$^+$ T cells, only a few dying cells were found, and the beads bound firmly to several living CD4$^+$ T cells (Fig. 5B). Anti-HLA-DR mAb abrogated the supportive effect of purified exosomes on naive CD4$^+$ T cell survival (Fig. 5C). Anti-HLA-DR mAb also inhibited the binding of exosome-coupled beads to naive CD4$^+$ T cells (data not shown).

3.4. Exosomes induce NF-κB activation in naive CD4$^+$ T cells

We hypothesized that interaction between HLA-DR on exosomes and TCRs on CD4$^+$ T cells induces NF-κB activation, and, as a result, these cells can survive even in severe culture conditions. NF-κB activation of naive CD4$^+$ T cells was estimated by EMSA. Crude exosomes induced NF-κB activation in naive CD4$^+$ T cells within 30 min. Specificity of DNA binding was confirmed by a competition study with a 50-fold excess of unlabeled oligonucleotide. Anti-HLA-DR mAb (4 μg/ml) was added to crude exosomes 1 h prior to coculture with naive CD4$^+$ T cells. Treatment with anti-HLA-DR mAb suppressed exosome-induced NF-κB activation. A NF-κB inhibitor, PDTC (100 μM), was added to naive CD4$^+$ T cells 1 h prior to treatment with crude exosomes. PDTC inhibited nuclear translocation of NF-κB p65 (Fig. 6). PDTC inhibited the supportive effect of crude exosomes on naive CD4$^+$ T cell survival in a dose-dependent manner between 3 and 5 μM without significant direct cytotoxic effect (Fig. 7). These data suggest that exosome-induced NF-κB activation plays a critical role in the survival of naive CD4$^+$ T cells in vitro.
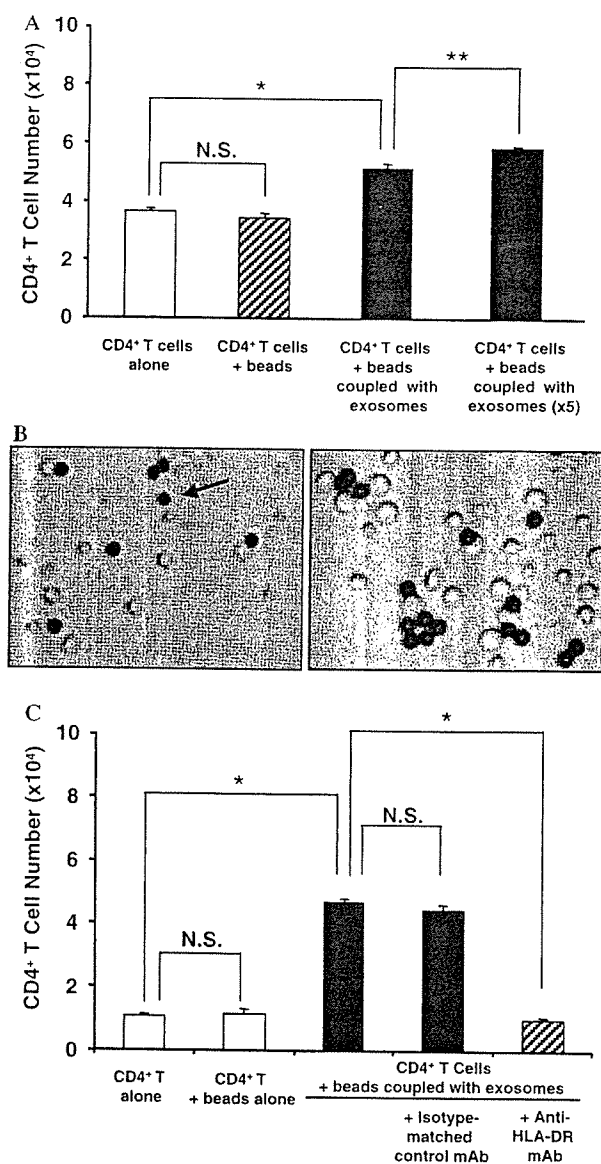
Fig. 5. Prolonged survival of naive CD4+ T cells by interaction with exosomes coupled to anti-MHC class II mAb-coated beads. (A) Viable cell numbers of naive CD4+ T cells cultured with exosomes coupled to anti-MHC class II mAb-coated beads (closed column) for 5 days are shown. Viable cell numbers of CD4+ T cells alone (open column) and CD4+ T cells with anti-HLA-DR mAb-coated beads only (hatched column) are also shown. The asterisk indicates significant differences <0.0001 (*) and 0.0029 (**). N.S. shows not significant. The data are representative of three independent experiments using Mo-DCs and CD4+ T cells obtained from three different healthy donors. (B) Phase-contrast photomicrographs of CD4+ T cells 5 days after coculture with beads (arrow) alone (left panel) and beads coupled with exosomes (right panel). The pictures are representative of three independent experiments using Mo-DCs and CD4+ T cells obtained from three different healthy donors. (C) Viable cell numbers of CD4+ T cells cultured with exosome-coupled beads in the presence (hatched column) or the absence (closed column) of anti-HLA-DR mAb or in the presence (closed column) of isotype-matched control mAb. Open column shows the viable cell number of CD4+ T cells alone and CD4+ T cells cultured with beads alone. The asterisk indicates significant differences <0.0001. N.S. shows not significant. Values represent means ± SD of triplicate determinations. The data are representative of three independent experiments using Mo-DCs and CD4+ T cells obtained from three different healthy donors.
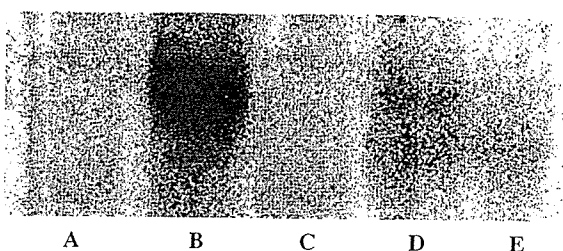

Fig. 6. NF-κB activation in naive CD4+ T cells induced by crude exosomes. The nuclear translocation of NF-κB p65 of naive CD4+ T cells in response to exosomes was determined by EMSA. Naive CD4+ T cells were incubated for 30 min for various conditions as below. Lane A, medium only; lane B, crude exosomes; lane C, crude exosomes with NF-κB ODN (50×); lane D, crude exosomes with anti-HLA-DR mAb; and lane E, crude exosomes with PDTC (100 μM). The data are representative of three independent experiments using Mo-DCs and CD4+ T cells obtained from three different healthy donors.
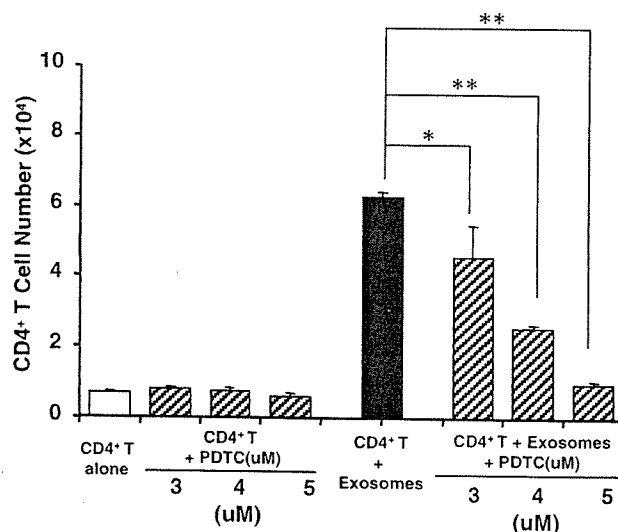

Fig. 7. Suppression of exosome-induced prolonged survival of naive CD4+ T cells by NF-κB inhibitor PDTC. Viable cell numbers of naive CD4+ T cells cultured with crude exosomes (closed column), crude exosomes with indicated concentrations of PDTC (hatched column) or medium alone (open column) for 5 days are shown. The asterisks indicate significant differences 0.0016 (*), <0.0001 (**). Values represent means ± SD of triplicate determinations. The data are representative of three independent experiments using Mo-DCs and CD4+ T cells obtained from three different healthy donors.

4. Discussion

We showed that Mo-DC-derived exosomes can prolong naive CD4+ T cell survival in an HLA-DR-dependent manner. Our data also suggest that NF-κB activation induced by exosomes contributes to this increased survival.

Several players such as TCRs and CD28 are related to T cell survival [5,30]. In the last two decades, many in vivo studies in mice have shown that long-term survival of naive CD4+ T cells requires interaction with self-MHC class II proteins [1–3]. However, it remains

unclear whether interaction with these proteins can prolong the short-term survival of naive CD4$^+$ T cells in vitro. Recently, it was shown that human Mo-DCs expressing abundant MHC class II proteins are able to support short-term survival of T cells in vitro [7]. Interestingly, our present findings indicate that although HLA-DR is critical for naive CD4$^+$ T cell survival in vitro (Fig. 3A), direct interaction between Mo-DCs and T cells is not always required (Fig. 2A). It has been shown that MHC class II proteins are very abundant in exosomes from APCs [10]. In the present study, Mo-DCs also released exosomes into culture medium, and Mo-DC-derived exosomes expressed both MHC class II and CD86 proteins (Fig. 4A). Recently, it was reported that MHC class II proteins on released exosomes are functional [10,31]. Raposo et al. [10] showed that exosomes derived from both human and murine B lymphocytes induce antigen-specific MHC class II-restricted T cell responses. Vincent-Schneider et al. [31] showed that the combination of exosomes with DCs results in highly efficient stimulation of specific T cells and suggested that exosome-bearing MHC class II complexes are taken up by dedicated APCs for efficient T cell activation. On the basis of these findings, we hypothesized that Mo-DC-derived exosomes can prolong naive CD4$^+$ T cell survival. To prove this, we used exosomes purified with human anti-HLA-DP, -DQ, or -DR-coated paramagnetic beads. To avoid contamination with serum-derived exosomes [32], we used RPMI 1640 medium supplemented with 1% human albumin. Purified exosomes prolonged naive CD4$^+$ T cell survival in an HLA-DR-dependent manner (Fig. 5C).

The present study shows a novel function of exosomes. Mo-DC-derived exosomes express not only MHC class II but also CD86 proteins. CD28, which is a ligand for CD86, is believed to contribute to T cell survival [29]. In our study, peripheral monocytes, in which CD86 expression is weak, did not prolong CD4$^+$ T cell survival (data not shown), suggesting a possible role of a CD28/CD86 interaction. But our data that specific antibody against HLA-DR inhibited completely the effect of exosomes on CD4$^+$ T cell survival. These data indicate that TCR is a likely candidate for transmitting the viability signal. However, participation of other receptors for MHC class II such as LAG-3 has not been excluded [33]. Furthermore, other molecular events, such as CD28/CD86 interaction, in addition to the interaction between TCR and HLA-DR may operate in prolongation of CD4$^+$ T cell survival induced with exosomes. A role of exosome-bearing CD86 in CD4$^+$ T cell survival has not been reported, and the mechanism of exosome-induced, HLA-DR-dependent naive CD4$^+$ T cell survival is not clear. Several transcription factors such as Ets, NFAT, AP-1, and NF-κB have been shown to be activated by TCRs or CD28 [20]. Recent studies have indicated that NF-κB plays a key role in T cell survival. For example, it has been suggested that the PI3K/Akt pathway is important for the effects of both CD28 and IL-2R [23,34,35], and NF-κB is thought to be target of Akt [36,37]. More direct evidence that NF-κB contributes to T cell survival has been reported recently [22,26]. In p50−/− cRel−/− mice, which exhibit virtually no inducible κB site binding activity, an essential role of TCR-induced NF-κB was indicated in T cell survival [26]. In addition, NF-κB regulated TCR-induced expression of anti-apoptotic Bcl-2 family members and NF-κB activation was not only necessary but was also sufficient for T cell survival [38]. Wan and DeGregon [22] reported that the survival of antigen-stimulated T cells requires NF-κB-mediated inhibition of p73 expression. Our present data show for the first time that Mo-DC-derived exosomes can induce NF-κB activation in naive CD4$^+$ T cells (Fig. 6). PDTC is a stable analog of dithiocarbamate and is one of the most widely used inhibitors of NF-κB signaling [39]. Although it has been postulated that PDTC acts simply as an antioxidant to inhibit NF-κB activation [40], it has been shown definitively that PDTC inhibits NF-κB activation independently of antioxidative function [41]. In the present study, we used PDTC to examine contribution of the NF-κB pathway to exosome-mediated CD4$^+$ T cell survival. PDTC inhibited the supportive effect of exosomes on CD4$^+$ T cell survival in a dose-dependent manner without significant direct cytotoxic effect (Fig. 7). These results suggest that NF-κB plays an essential role in exosome-mediated CD4$^+$ T cell survival. However, we have no definitive evidence as to how exosomes induce NF-κB in naive CD4$^+$ T cells.

It has been reported that DC-derived exosomes may be used as vectors for vaccination because they express high levels of functional MHC class I– and class II–peptide complexes, together with CD86 [10,14,19]. A recent report showed that MHC class I proteins on purified exosomes from DCs can be directly loaded with peptide at much greater levels than by indirect loading [17]. Also reported was a new exosome purification procedure from Mo-DCs [14], in which ultrafiltration through a 500-kDa membrane and ultracentrifugation into a 30% sucrose/deuterium-oxide cushion made it possible to recover up to 50% exosomes. Although the function of most of the exosome-bearing proteins is unknown at present, accumulated data on exosome function suggest that these proteins will become exciting therapeutic tools in the near future.

Acknowledgments

References

[1] S. Takeda, H.R. Rodewald, H. Arakawa, H. Bluethmann, T. Shimizu, MHC class II molecules are not required for survival of newly generated CD4$^+$ T cells, but affect their long-term life span, Immunity 5 (1996) 217–228.

[2] T. Brocker, Survival of mature CD4 T lymphocytes is dependent on major histocompatibility complex class II-expressing dendritic cells, J. Exp. Med. 186 (1997) 1223–1232.

[3] S. Garcia, J. DiSanto, B. Stockinger, Following the development of a CD4 T cell response in vivo: from activation to memory formation, Immunity 1 (1999) 163–171.

[4] C. Tanchot, F.A. Lemonnier, B. Perarnau, A.A. Freitas, B. Rocha, Differential requirements for survival and proliferation of CD8 naive or memory T cells, Science 276 (1997) 2057–2062.

[5] J. Kirberg, A. Berns, H. von Boehmer, Peripheral T cell survival requires continual ligation of the T cell receptor to major histocompatibility complex-encoded molecules, J. Exp. Med. 186 (1997) 1269–1275.

[6] C. Viret, F.S. Wong, C.A. Janeway Jr., Designing and maintaining the mature TCR repertoire: the continuum of self-peptide:self-MHC complex recognition, Immunity 10 (1999) 559–568.

[7] T. Kondo, I. Cortese, S. Markovic-Plese, K.P. Wandinger, C. Carter, M. Brown, S. Leitman, R. Martin, Dendritic cells signal T cells in the absence of exogenous antigen, Nat. Immunol. 2 (2001) 932–938.

[8] E.G. Trams, C.J. Lauter, N. Salem Jr., U. Heine, Exfoliation of membrane ecto-enzymes in the form of micro-vesicles, Biochim. Biophys. Acta 645 (1981) 63–70.

[9] R.M. Johnstone, M. Adam, J.R. Hammond, L. Orr, C. Turbide, Vesicle formation during reticulocyte maturation. Association of plasma membrane activities with released vesicles (exosomes), J. Biol. Chem. 262 (1987) 9412–9420.

[10] G. Raposo, H.W. Nijman, W. Stoorvogel, R. Liejendekker, C.V. Harding, C.J. Melief, H.J. Geuze, B lymphocytes secrete antigen-presenting vesicles, J. Exp. Med. 183 (1996) 1161–1172.

[11] J.Q. Davis, D. Dansereau, R.M. Johnstone, V. Bennett, Selective externalization of an ATP-binding protein structurally related to the clathrin-uncoating ATPase/heat shock protein in vesicles containing terminal transferrin receptors during reticulocyte maturation, J. Biol. Chem. 261 (1986) 15368–15371.

[12] C. Thery, M. Boussac, P. Veron, P. Ricciardi-Castagnoli, G. Raposo, J. Garin, S. Amigorena, Proteomic analysis of dendritic cell-derived exosomes: a secreted subcellular compartment distinct from apoptotic vesicles, J. Immunol. 166 (2001) 7309–7318.

[13] F. Sallusto, A. Lanzavecchia, Efficient presentation of soluble antigen by cultured human dendritic cells is maintained by granulocyte/macrophage colony-stimulating factor plus interleukin 4 and downregulated by tumor necrosis factor alpha, J. Exp. Med. 179 (1994) 1109–1118.

[14] L. Zitvogel, A. Regnault, A. Lozier, J. Wolfers, C. Flament, D. Tenza, P. Ricciardi-Castagnoli, G. Raposo, S. Amigorena, Eradication of established murine tumors using a novel cell-free vaccine: dendritic cell-derived exosomes, Nat. Med. 4 (1998) 594–600.

[15] H.G. Lamparski, A. Metha-Damani, J.Y. Yao, S. Patel, D.H. Hsu, C. Ruegg, J.B. Le Pecq, Production and characterization of clinical grade exosomes derived from dendritic cells, J. Immunol. Methods 270 (2002) 211–226.

[16] C. Thery, L. Duban, E. Segura, P. Veron, O. Lantz, S. Amigorena, Indirect activation of naive CD4$^+$ T cells by dendritic cell-derived exosomes, Nat. Immunol. 3 (2002) 1156–1162.

[17] D.H. Hsu, P. Paz, G. Villaflor, A. Rivas, A. Mehta-Damani, E. Angevin, L. Zitvogel, J.B. Le Pecq, Exosomes as a tumor vaccine: enhancing potency through direct loading of antigenic peptides, J. Immunother. 26 (2003) 440–450.

[18] I. Hwang, X. Shen, J. Sprent, Direct stimulation of naive T cells by membrane vesicles from antigen-presenting cells: distinct roles for CD54 and B7 molecules, Proc. Natl. Acad. Sci. USA 100 (2003) 6670–6675.

[19] D. Skokos, H.G. Botros, C. Demeure, J. Morin, R. Peronet, G. Birkenmeier, S. Boudaly, S. Mecheri, Mast cell-derived exosomes induce phenotypic and functional maturation of dendritic cells and elicit specific immune responses in vivo, J. Immunol. 170 (2003) 3037–3045.

[20] C.T. Kou, J.M. Leiden, Transcriptional regulation of T lymphocyte development and function, Annu. Rev. Immunol. 17 (1999) 149–187.

[21] E. Dudley, F. Hornung, L. Zheng, D. Scherer, D. Ballard, M. Lenardo, NF-kappaB regulates Fas/APO-1/CD95- and TCR-mediated apoptosis of T lymphocytes, Eur. J. Immunol. 29 (1999) 878–886.

[22] Y.Y. Wan, J. DeGregon, The survival of antigen-stimulated T cells requires NFkappaB-mediated inhibition of p73 expression, Immunity 18 (2003) 331–342.

[23] R.G. Jones, M. Parsons, M. Bonnard, V.S. Chan, W.C. Yeh, J.R. Woodgett, P.S. Ohashi, Protein kinase B regulates T lymphocyte survival, nuclear factor kappaB activation, and Bcl-X(L) levels in vivo, J. Exp. Med. 191 (2000) 1721–1734.

[24] S. Ghosh, M.J. May, E.B. Kopp, NF-kB and Rel proteins: evolutionarily conserved mediators of immune responses, Annu. Rev. Immunol. 16 (1998) 225–260.

[25] J.A. DiDonato, F. Mercurio, M. Karin, Phosphorylation of IkB precedes but is not sufficient for its dissociation from NF-kB, Mol. Cell. Biol. 15 (1995) 1302–1311.

[26] Y. Zheng, M. Vig, J. Lyons, L. Van Parijs, A.A. Bed, Combined deficiency of p50 and cRel in CD4$^+$ T cells reveals an essential requirement for nuclear factor kappa B in regulating mature T cell survival and in vivo function, J. Exp. Med. 197 (2003) 861–874.

[27] M. Kojima, T. Morisaki, K. Izuhara, A. Uchiyama, Y. Matsunari, M. Katano, M. Tanaka, Lipopolysaccharide increase cyclooxygenase-2 expression in a colon carcinoma cell line through nuclear factor-kappa B activation, Oncogene 19 (2000) 1225–1231.

[28] J.A. Hobot, E. Carlemalm, W. Villiger, E. Kellenberger, Periplasmic gel: new concept resulting from the reinvestigation of bacterial cell envelope ultrastructure by new methods, J. Bacteriol. 160 (1984) 143–152.

[29] A. Clayton, J. Court, H. Navabi, M. Adams, M.D. Mason, J.A. Hobot, G.R. Newman, B. Jasani, Analysis of antigen presenting cell derived exosomes, based on immuno-magnetic isolation and flow cytometry, J. Immunol. Methods 247 (2001) 163–174.

[30] L.H. Boise, A.J. Minn, P.J. Noel, C.H. June, M.A. Accavitti, T. Lindsten, C.B. Thompson, CD28 costimulation can promote T cell survival by enhancing the expression of Bcl-XL, Immunity 3 (1995) 87–98.

[31] H. Vincent-Schneider, P. Stumptner-Cuvelette, D. Lankar, S. Pain, G. Raposo, P. Benaroch, C. Bonnerot, Exosomes bearing HLA-DR1 molecules need dendritic cells to efficiently stimulate specific T cells, Int. Immunol. 14 (2002) 713–722.

[32] G. van Niel, G. Raposo, C. Candalh, M. Boussac, R. Hershberg, N. Cerf-Bensussan, M. Heyman, Intestinal epithelial cells secrete exosome-like vesicles, Gastroenterology 121 (2001) 337–349.

[33] C.J. Workman, D.A. Vignali, The CD4-related molecule, LAG-3 (CD223), regulates the expansion of activated T cells, Eur. J. Immunol. 33 (2003) 970–979.

[34] J.S. Burr, N.D. Savage, G.E. Messah, S.L. Kimzey, A.S. Shaw, R.H. Arch, J.M. Green, Cutting edge: distinct motifs within CD28 regulate T cell proliferation and induction of Bcl-XL, J. Immunol. 166 (2001) 5331–5335.

[35] K.A. Frauwirth, J.L. Riely, M.H. Harris, R.V. Parry, J.C. Rathmell, D.R. Plas, R.L. Elstrom, C.H. June, C.B. Thompson, The CD28 signaling pathway regulates glucose metabolism, Immunity 16 (2002) 769–777.

[36] L.P. Kane, V.S. Shapiro, D. Stokoe, A. Weiss, Induction of NF-kappaB by the Akt/PKB kinase, Curr. Biol. 9 (1999) 601–604.

[37] J.A. Romashkova, S.S. Makarov, NF-kappaB is a target of AKT in anti-apoptotic PDGF signaling, Nature 401 (1999) 86–90.

[38] R.J. Grumont, I.J. Rourke, S. Gerondakis, Rel-dependent induction of A1 transcription is required to protect B cells from antigen receptor ligation-induced apoptosis, Genes Dev. 13 (1999) 400–411.

[39] P.A. Baeuerle, T. Henkel, Function and activation of NF-kB in the immune system, Annu. Rev. Immunol. 12 (1994) 141–179.

[40] L. Flohe, R. Brigelius-Flohe, C. Saliou, M.G. Traber, L. Packer, Redox regulation of NF-kappa B activation, Free Radic. Biol. Med. 22 (1997) 1115–1126.

[41] M. Hayakawa, H. Miyashita, I. Sakamoto, M. Kitagawa, H. Tanaka, H. Yasuda, M. Karin, K. Kikugawa, Evidence that reactive oxygen species do not mediate NF-kB activation, EMBO J. 22 (2003) 3356–3366.

ORIGINAL ARTICLE

Hiroshi Nakashima · Akira Tasaki · Makoto Kubo
Hideo Kuroki · Kotaro Matsumoto · Masao Tanaka
Masafumi Nakamura · Takashi Morisaki
Mitsuo Katano

Effects of docetaxel on antigen presentation-related functions of human monocyte-derived dendritic cells

Abstract *Purpose*: Docetaxel (TXT) is a unique chemotherapeutic agent that has been approved for treating various types of malignancies. TXT stabilizes microtubule assembly in cells and causes various dysfunctions of microtubule-dependent cellular events. Patients with advanced malignancies are beginning to receive TXT in combination with immunotherapy; however, the influence of TXT at clinically achievable serum concentrations (less than 10^{-6} *M*) on antigen presentation-related functions of human monocyte-derived dendritic cells (Mo-DCs) remains unclear. *Methods*: Immature Mo-DCs (imMo-DCs) were generated from peripheral blood monocytes with interleukin-4 and granulocyte-macrophage colony-stimulating factor in vitro. Mature Mo-DCs (mMo-DCs) were induced from imMo-DCs with tumor necrosis factor-α and prostaglandin E_2. *Results*: TXT at concentrations lower than 10^{-7} *M* did not significantly affect cellular viability, phagocytosis, or expression of antigen presentation-related molecules of Mo-DCs. In contrast, TXT at concentrations lower than 10^{-9} *M* significantly suppressed directional motility of imMo-DCs toward MIP-1α and of mMo-DCs toward MIP-3β. However, TXT had no effect on either CCR1 expression by imMo-DCs or CCR7 expression by mMo-DCs. No gross changes in the microtubule skeleton were evident by immunofluorescence microscopy after treatment with TXT at less than 10^{-8} *M*. However, reduced numbers of imMo-DCs with podosomes localized primarily in one cell region were observed. *Conclusions*: The present results indicate that different concentrations of TXT influence antigen presentation-related functions differently. In particular, TXT at relatively low therapeutic doses disrupts chemotactic motility of Mo-DCs.

Keywords Taxane · Non-directional migration · Directional migration · Microtubules · Immunotherapy

H. Nakashima · A. Tasaki · M. Kubo · H. Kuroki
K. Matsumoto · M. Nakamura · T. Morisaki
M. Katano (✉)
Department of Cancer Therapy and Research,
Graduate School of Medical Sciences,
Kyushu University, 3-1-1 Maidashi,
Higashiku, Fukuoka City 812-8582, Japan
E-mail: mkatano@tumor.med.kyushu-u.ac.jp
Tel.: +81-92-6426941
Fax: +81-92-6426221

M. Tanaka
Department of Surgery and Oncology,
Graduate School of Medical Sciences,
Kyushu University, 3-1-1 Maidashi,
Higashiku, Fukuoka City 812-8582, Japan

Introduction

Dendritic cells (DCs) are the most potent antigen-presenting cells (APCs) and are capable of inducing primary sensitization against specific antigens in naive T cells [3]. Immature DCs (imDCs) exist in most tissues. They capture and process antigens. Following activation, they display these antigens in the form of MHC-peptide complexes at their surface [9]. Mature DCs (mDCs) enter lymphatic vessels, migrate to T-dependent areas of secondary lymphoid organs, and stimulate naive T cells [2]. Thus, the ability of DCs to migrate is crucial to the transmission of immunological events in peripheral tissues to secondary lymphoid organs.

It is now possible to generate in vitro DC-like APCs (Mo-DCs) from human peripheral blood mononuclear cells (PBMCs) with granulocyte-macrophage colony-stimulating factor (GM-CSF) and interleukin-4 (IL-4) [29]. Immature Mo-DCs (imMo-DCs) and mature Mo-DCs (mMo-DCs) also migrate toward MIP-1α and MIP-3β, respectively [8, 22]. Mature Mo-DCs are able to enter lymphatic vessels and migrate to regional lymph nodes in animal models, and mMo-DCs might be involved in induction of tumor-specific cytotoxic T lymphocytes (CTLs) [11, 44]. Based on these experimental findings, a number of studies have shown that

subcutaneous injection of mMo-DCs loaded with tumor-associated antigens leads to antitumor immune responses in patients with various types of malignancies [4, 11, 13, 28]. In these DC-based vaccine therapies, the ability of injected mMo-DCs to migrate plays an essential role in CTL induction.

For a cell to invade, the front of the cell must protrude and attach to a substrate and then the rear part of the cell must be able to retract. These processes are directly driven by the actin cytoskeleton [35, 36]. Podosomes are unique actin-rich adhesion structures of monocyte-derived cells [7]. They are highly dynamic and actively engage in matrix remodeling and tissue invasion [25]. Microtubules also play a role in the locomotion of most, but not all, cell types, and they may be involved in the coordination of the direction of cell movement [15, 33]. Linder et al. [26] have shown that microtubules are essential for podosome formation in primary human macrophages. These findings indicate the significance of actin and microtubule cytoskeletons in cell motility. Thus, compounds that damage actin or microtubules may affect cell motility.

Docetaxel (TXT) is a new chemotherapeutic agent that has been approved for treatment of various types of malignancies [16, 18–20, 23, 30]. TXT is a semisynthetic taxane derived from the needles of the European yew (*Taxus baccata*). It binds to tubulin, leading to microtubule stabilization, mitotic arrest, and subsequent cell death [14, 17, 39]. TXT has been reported to affect the migratory capacity of certain cells such as endothelial cells [21], smooth muscle cells [1], some cancer cells [5, 37, 40], and neutrophils [32]. However, there is limited information concerning the influence of TXT on Mo-DC motility.

Cancer patients receiving chemotherapeutic agents, including TXT, sometimes also receive DC vaccine therapy. In addition, recent animal experiments suggest that chemotherapeutic agents administered in combination with Mo-DC-based vaccine therapy may be effective for treating cancer patients with multiple drug resistance [41]. Thus DC vaccine therapy is likely to become a more common component in regimens for treatment of cancer. Because TXT affects microtubule function, which is important for motility of DCs used in vaccine therapy, we investigated the effect of TXT on immunological functions of Mo-DCs, with particular emphasis on Mo-DC motility.

Materials and methods

Reagents and antibodies

TXT was purchased from Rhone-Poulenc-Rorer (Antony, France). Streptococcal preparation OK-432 was provided by Chugai Pharmaceutical Company (Tokyo, Japan). Human MIP-1α and MIP-3β were purchased from Diaclone Research (Besançon, France). The following monoclonal antibodies (mAb), conjugated with either fluorescein isothiocyanate (FITC) or phycoerythrin (PE), were purchased from BD Biosciences Pharmingen (San Diego, Calif.): CD14, CD80, CD83, CD86, HLA-DR. Unlabeled mouse anti-human CCR1 and CCR7, FITC-conjugated gout anti-mouse immunoglobulins, and isotype controls, IgG1 and IgG2a, were also purchased from BD Biosciences Pharmingen.

Mo-DC preparation

Mo-DCs were generated from the PBMCs of healthy volunteers as previously described with minor modifications [43]. Briefly, PBMCs were suspended in RPMI 1640 medium (Sanko Pure Chemicals, Tokyo, Japan) with 10% fetal calf serum (FCS) (referred to as RPMI-FCS medium) for 4 h at 37°C, and the adherent cells were cultured in RPMI medium supplemented with 200 ng/ml GM-CSF (GeneTech, Beijing, China) and 500 U/ml IL-4 (Osteogenetics, Würzburg, Germany). On day 7, non-adherent cells were collected and further purified by negative selection with magnetic beads coated with mouse monoclonal anti-CD2, anti-CD3, and anti-CD19 antibodies (Dynabeads, Dynal Biotech, Oslo, Norway). This depletion procedure yielded over 90% $CD14^-$, $CD80^+$, and $HLA-DR^+$ imMo-DCs as assessed by fluorescence-activated cell sorting (FACS) with a FACS Calibur (Becton Dickinson, Franklin Lakes, N.J.). To induce maturation, imMo-DCs were cultured with RPMI-FCS medium supplemented with tumor necrosis factor-α (TNF-α, 200 U/ml; Dainippon Pharmaceutical, Osaka, Japan) and prostaglandin E_2 (PGE$_2$, 1 μg/ml; Sigma, St. Louis, Mo.) for two additional days [27]. These cells were used as mMo-DCs [24].

Cell viability and detection of apoptosis

ImMo-DCs were seeded into 96-well plates and cocultured with the indicated concentrations of TXT at 37°C in RPMI 1640 supplemented with 1% human albumin (hereafter referred to as RPMI-Alb medium). Following incubation for 24 h, cell viability was determined by the 3-[4,5-dimethythiazol-2-yl] 2,5-diphenyltetrazolium bromide (MTT) assay. Percent cell viability is expressed as the mean ± SD of three independent wells.

Morphological changes in the nuclear chromatin of cells undergoing apoptosis were detected by staining with the membrane-permeable dye Hoechst 33342 (Wako Chemicals, Osaka, Japan). Briefly, cells were plated in 96-well plates, treated with TXT for 24 h, stained with Hoechst 33342, and then observed by fluorescence microscopy. A total of 300 cells were counted in three randomly chosen fields at ×100 magnification. Cells with condensed or fragmented nuclei were considered to be apoptotic. The proportions of apoptotic cells are

expressed as mean ± SD percentages of three independent wells.

Immunofluorescence microscopy

ImMo-DCs and mMo-DCs were pretreated with the indicated concentrations of TXT at 37°C for 24 h. After incubation, cells were washed with RPMI to eliminate TXT. Washed cells were allowed to adhere to glass coverslips at 37°C overnight. Cells were then fixed with 100% methanol at −20°C for 5 min. After washing with PBS containing 0.1% Tween 20 (Nacalai Tesque, Kyoto, Japan), non-specific binding was blocked with 10% goat serum in PBS. Actin and microtubule cytoskeleton were visualized by immunofluorescence staining with mouse mAbs to actin (1:200; Sigma) and to α-tubulin (1:500; Sigma), respectively. Alexa 594-conjugated goat anti-mouse IgG antibody (Wako Chemicals) was used as a second antibody. Fluorescence signals were detected with a Radiance 2000 confocal laser-scanning microscope (Bio-Rad Laboratories, Hercules, Calif.). Images were processed with Laser Sharp 2000 software (Bio-Rad Laboratories).

Migration of Mo-DCs

Migration of Mo-DCs was determined by counting the number of cells that migrated through Transwell inserts with filter membranes of pore size 8 mm (BD Biosciences Pharmingen). The effect of TXT on non-directional Mo-DC migration was determined as follows. Mo-DCs treated with designated doses of TXT for 24 h were suspended at a concentration of 2×10^5 cells/ml in RPMI-Alb medium. Cell suspension (500 μl) was added to the upper compartment, and RPMI-Alb medium (400 μl) was added to the lower compartment. The cells were incubated at 37°C for 6 h. After incubation, the filter was fixed with 100% methanol and stained with Giemsa solution, and the cells on the upper surface were completely removed. Mo-DCs that had migrated from the upper side to the lower side of the filter were counted under a light microscope at a magnification of ×200. Non-directional migration is expressed as the mean ± SD migrating cell number of five microscopic fields.

The procedure for determining the effect of TXT on directional migration was the same as that for determining non-directional migration; however, to determine directional migration of imMo-DCs or mMo-DCs, MIP-1α (10 ng/ml) or MIP-3β (100 ng/ml), respectively, was added to the lower compartment.

Chemokine-induced invasiveness of Mo-DCs

Chemokine-induced invasiveness of Mo-DCs was measured by the invasion of cells through Matrigel-coated Transwell inserts [42]. Briefly, the upper surface of the filter (pore size 8.0 μm; BD Biosciences Pharmingen) was coated with basement membrane Matrigel (BD Biosciences Pharmingen) at a concentration of 250 μg/cm² and air-dried overnight at room temperature. The invasion assay was similar to the directional migration assay described above. MIP-1α (for imMo-DCs) or MIP-3β (for mMo-DCs) was added to the lower compartment. After 24 h, Mo-DCs that had migrated from the upper side to the lower side of the filter were counted under a light microscope at a magnification of ×200. Chemokine-induced invasion is expressed as the mean ± SD migrating cell number of five microscopic fields.

Evaluation of phagocytosis

Immature Mo-DCs (1×10^5/well) pretreated with designated doses of TXT for 24 h were suspended in RPMI 1640 medium with FITC-conjugated dextran (FITC-DX, Sigma) and incubated for 12 h. The percentage of imMo-DCs that captured FITC-DX was determined by examining 100 imMo-DCs under a fluorescence microscope. The percent phagocytosis is expressed as the mean ± SD of three wells.

Alternatively, imMo-DCs were labeled with PE-conjugated anti-HLA-DR mAb. The fluorescence-labeled imMo-DCs were cultured with FITC-DX for 12 h at 37°C or 4°C, washed, and applied to a FACS Calibur flow cytometer. The fluorescence intensity was analyzed with CellQuest (Becton-Dickinson). FITC-positive cells in gated HLA-DR-positive imMo-DC populations were defined as dextran-captured imMo-DCs.

Expression of antigen presentation-related antigens of Mo-DCs

For analysis of the effect of TXT on expression of maturation-related molecules of Mo-DCs, the following mouse anti-human mAbs, conjugated with either FITC or PE, were used: CD14, CD80, CD83, CD86, and HLA-DR. Unlabeled mouse anti-human mAbs CCR1 and CCR7 were visualized with FITC-conjugated anti-mouse immunoglobulins. Isotype controls, IgG1, and IgG2a were also included. Cells were stained at a concentration of 1×10^5 in 100 μl. Samples were incubated with the conjugated mAbs for 60 min at 4°C and then washed twice with PBS containing 3% bovine serum albumin (BSA; Sigma) and 0.1% NaN_3 (Sigma). The samples were analyzed with a FACS Calibur flow cytometer and CellQuest.

IL-12 secretion in Mo-DCs

Because our previous study had shown that OK-432 induces IL-12 secretion in imMo-DCs [24, 31], imMo-DCs

$(1\times10^5/\text{ml})$ were incubated with the indicated doses of TXT for 24 h at 37°C, washed to eliminate TXT, and then incubated with OK-432 (0.02 KE/ml) for 24 h. Cell-free supernatants were collected by centrifugation and stored at −80°C. The concentration of IL-12 p40 and p70 in the supernatants was determined using an enzyme-linked immunosorbent assay (ELISA) kit specific for measuring IL-12 p40 and p70 (BioSource International, Camarillo, Calif.) according to the manufacturer's instructions. The detection limit for IL-12 p40 and p70 was 7.8 pg/ml and 1.56 pg/ml, respectively. Concentrations of IL-12 p40 are expressed as the mean ± SD of the data from three independent experiments.

Mixed lymphocyte reaction

Mixed lymphocyte reaction (MLR) was carried out in U-bottomed 96-well plates with a total volume of 200 µl per well. Irradiated imMo-DCs (2×10^4 cells), which were treated with designated doses of TXT for 24 h at 37°C, were suspended in RPMI-Alb medium. Allogenic PBMCs (1×10^5) were used as responders. Wells were pulsed 3 days after the initial culture with 1 µCi (0.037 MBq) of [³H]-thymidine (Amersham Pharmacia Biotech, Piscataway, N.J.). [³H]-Thymidine incorporation was measured 24 h after the addition of [³H]-thymidine with a liquid-scintillation counter (Beckman Coulter, Palo Alto, Calif.). [³H]-Thymidine uptake is expressed as the mean ± SD counts per minute of three wells.

Statistical analysis

Statistical analysis was performed with the unpaired two-tailed Student's t test; $P < 0.05$ was considered significant.

Results

Effects of TXT on the viability of Mo-DCs

Achievable serum concentrations of TXT in the clinical setting are lower than 10^{-6} M and a concentration of 10^{-9} M is maintained for about 72 h [6]. When imMo-DCs were exposed to TXT at concentrations greater than 10^{-6} M for 24 h, viability decreased (Fig. 1a). The pattern of cellular death was apoptosis (Fig. 1b). Data are representative of six independent experiments with imMo-DCs generated from three different healthy donors.

Effects of TXT on cytoskeletal organization of imMo-DCs

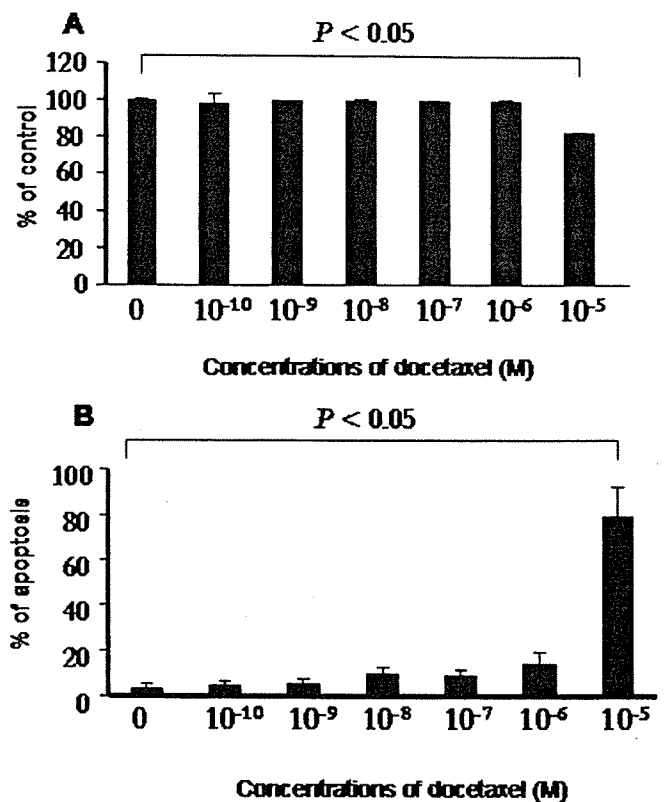Untreated imMo-DCs were oval in shape, indicating a polarized morphology (Fig. 2a). After treatment with

Fig. 1 Effect of TXT on viability of imMo-DCs. a The MTT assay was performed after 24 h of TXT treatment. Each experiment was performed in triplicate and the average optical density (OD) at 570 nm was calculated. The data presented are the means ± SD of three different wells. b Cells were stained with Hoechst 33342 and examined by fluorescence microscopy. A total of 300 cells were counted in three randomly chosen fields at ×100 magnification. Cells with condensed or fragmented nuclei were considered to be apoptotic. The data presented are percent apoptosis and are the means ± SD of three independent wells

TXT at concentrations greater than 10^{-8} M, imMo-DCs became rounded (Fig. 2d). The effect of TXT on cytoskeletal organization was examined by immunohistochemistry as described in "Materials and methods" (Fig. 2). In more than 90% of untreated imMo-DCs, multiple clear small actin foci resembling podosomes were found (Fig. 2b). Clusters of podosomes were localized primarily to one region in most untreated imMo-DCs, whereas in about 70% of imMo-DCs treated with TXT at 10^{-8} M, podosome clustering was mostly absent (Fig. 2e). In particular, almost all imMo-DCs treated with TXT at concentrations greater than 10^{-7} M failed to spread significantly on Matrigel-coated glass coverslips and lacked podosomes (Fig. 2h). No apparent change in microtubule cytoskeleton was found in cells treated with concentrations lower than 10^{-8} M TXT (Fig. 2f); however, an interwoven fabric of highly concentrated filaments or dense peripheral banding of filaments was found in almost all cells treated with greater than 10^{-7} M TXT (Fig. 2i).

Fig. 2 Effect of TXT on cytoskeletal organization of imMo-DCs. ImMo-DCs were treated with the indicated doses of TXT for 24 h and observed under a phase contrast microscope (a, d, g; ×400) and confocal laser microscope (b, c, e, f, h, i; ×2000). Specimens were stained with either anti-actin mAb (b, e, h) or anti-α-tubulin mAb (c, f, i). *Arrows* indicate podosomes

Concentrations of TXT
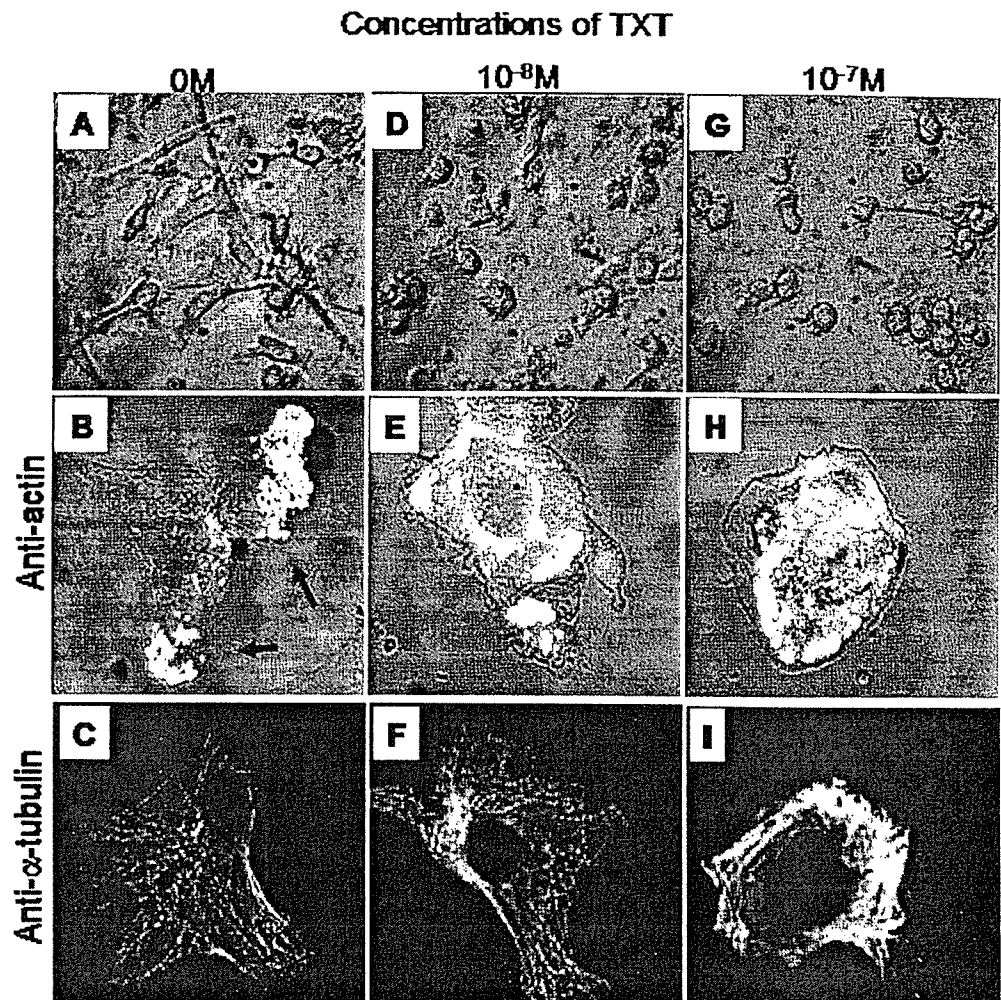
Effects of TXT on the motility of Mo-DCs

A migration assay was performed with a modified Boyden chamber technique as described in "Materials and methods". TXT at 10^{-8} M significantly decreased non-directional motility of both imMo-DCs and mMo-DCs (Fig. 3a,b). TXT at 10^{-10} M significantly decreased MIP-1α-induced directional motility of imMo-DCs (Fig. 3c), and TXT at 10^{-9} M significantly decreased MIP-3β-induced directional motility of mMo-DCs (Fig. 3d). The data presented are representative of three independent experiments with Mo-DCs generated from three different healthy donors.

Because CCR1 and CCR7 are receptors for MIP-1α and MIP-3β, respectively [8], we examined by FACS analysis the effect of TXT on expression of CCR1 on imMo-DCs and CCR7 on mMo-DCs. TXT at concentrations lower than 10^{-7} M did not significantly affect the expression CCR1 and CCR7 on Mo-DCs (data not shown).

Effect of TXT on chemokine-induced invasiveness of Mo-DCs

To invade a new territory, Mo-DCs must be able to penetrate the matrix, especially in response to chemokines. In this study, chemokine-induced invasive ability (chemo-invasive ability) was determined by a Matrigel invasion assay as described in "Materials and methods". TXT at 10^{-9} M significantly decreased the chemoinvasive ability of imMo-DCs or mMo-DCs toward MIP-1α or MIP-3β, respectively (Fig. 4a,b). The data presented are representative of three independent experiments with Mo-DCs generated from three different healthy donors.

Effect of TXT on phagocytic activity of Mo-DCs

Phagocytic ability of imMo-DCs was determined with FITC-DX by both fluorescence microscopy (data not

484

Fig. 3 Effect of TXT on the
motility of Mo-DCs. The data
presented are the ratios of
TXT-treated migrating Mo-
DCs to untreated Mo-DCs. a
Non-directional migration of
imMo-DCs; b non-directional
migration of mMo-DCs; c
directional migration of imMo-
DCs against MIP-1α; d
directional migration of mMo-
DCs against MIP-3β

shown) and FACS analysis (Fig. 5) as described in "Materials and methods". TXT at concentrations lower than 10^{-7} M did not affect phagocytic ability of imMo-DCs (Fig. 5). The data presented are representative of three independent experiments with Mo-DCs generated from three different healthy donors. When imMo-DCs were cultured with FITC-DX at 4°C (Fig. 5), their phagocytic ability was less than 5%, indicating capture of dextran by imMo-DCs rather than non-specific binding of dextran with imMo-DCs.
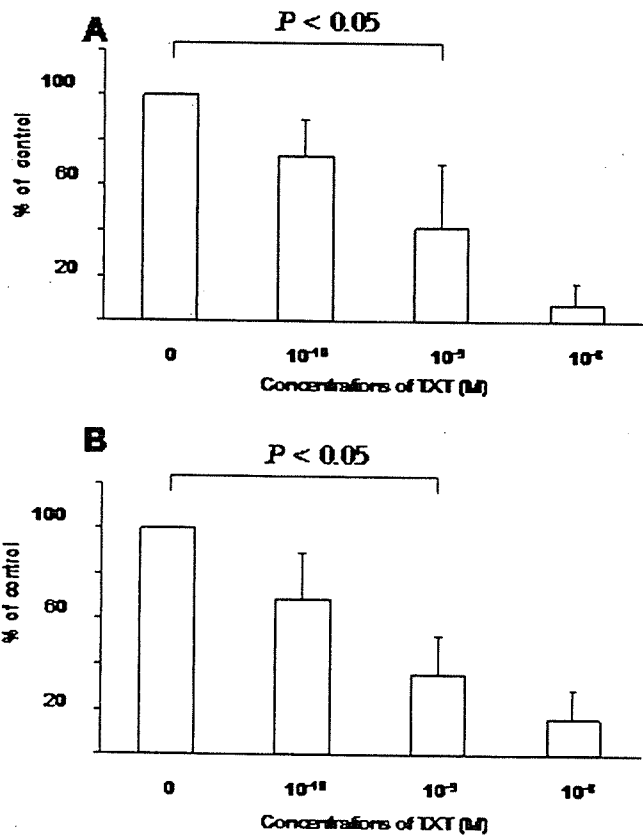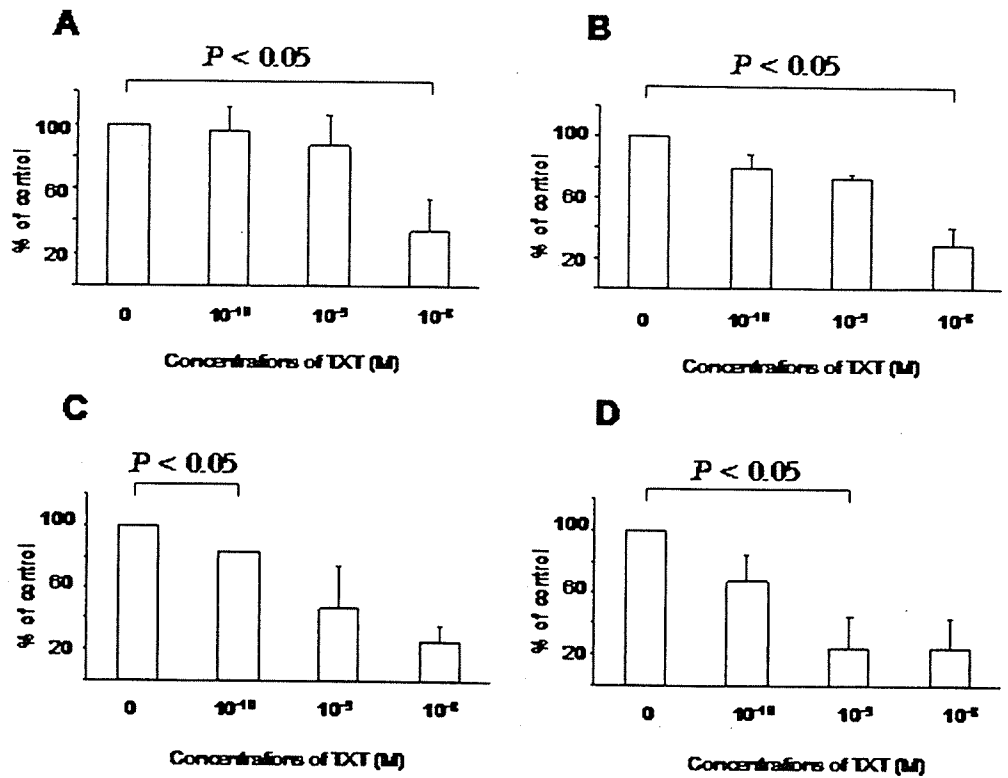
Fig. 4 Effect of TXT on chemoinvasive ability of Mo-DCs as determined by a Matrigel invasion assay. The data presented are the ratios of TXT-treated migrating Mo-DCs to untreated Mo-DCs. a Chemokine-induced invasion of imMo-DCs toward MIP-1α; b chemokine-induced invasion of mMo-DCs toward MIP-3β
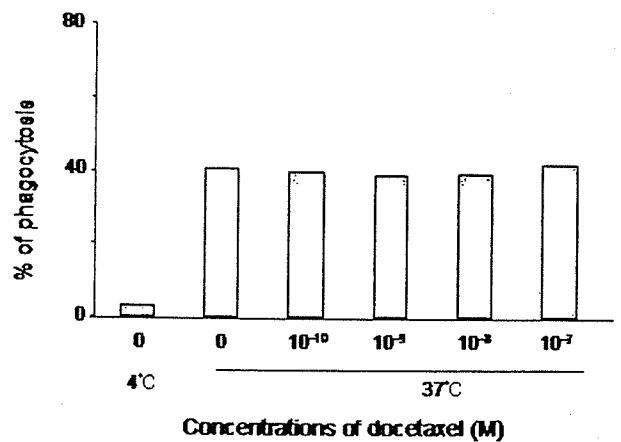
Fig. 5 Effect of TXT on phagocytosis by imMo-DCs. Cells were cocultured for 12 h with FITC-DX and subjected to FACS analysis. The data presented are representative of three different experiments
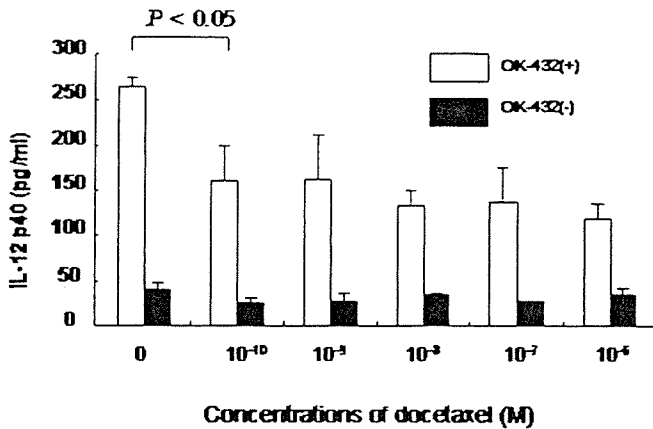
Fig. 6 Effect of TXT on IL-12 production by OK-432-stimulated Mo-DCs. ImMo-DCs treated with the indicated doses of TXT for 24 h were incubated with or without 0.02 KE/ml OK-432 at 37°C for 24 h. IL-12 p40 concentrations in the culture medium were determined by ELISA. The data presented are the means±SD of three different wells

Effect of TXT on the expression of antigen presentation-related antigens of Mo-DC

TXT at 10^{-7} M did not affect the expression of antigen presentation-related antigens, including CD14, HLA-DR, CD80, and CD83, on either imMo-DCs or mMo-DCs (data not shown).

Effect of TXT on IL-12 production by Mo-DCs

When imMo-DCs capture antigens, such as strepto-coccal preparation OK-432, they secrete IL-12, which plays an important role in induction of CTLs [38]. Based on this finding, we examined the effect of TXT on IL-12 p40 production by imMo-DCs stimulated
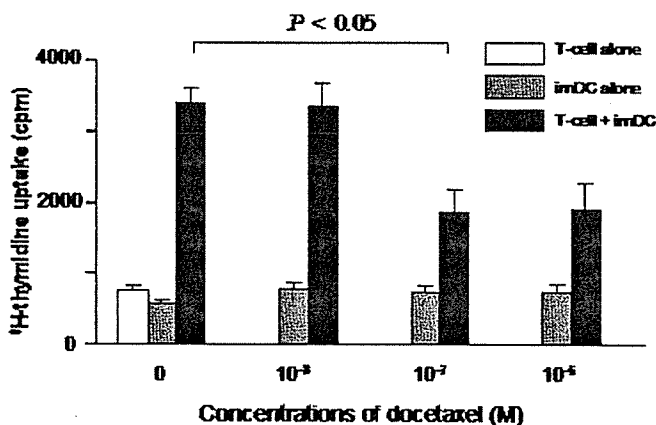

Fig. 7 Effect of TXT on allogenic T-cell stimulation by imMo-DCs. [³H]-Thymidine incorporation into allogenic T cells cultured with TXT-treated imMo-DCs is shown. The data presented are the means±SD of three different wells

with OK-432. TXT at 10^{-10} M reduced IL-12 p40 production of imMo-DCs (Fig. 6) after coincubation with OK-432, but IL-12 p40 production from imMo-DCs without OK-432 stimulation was not affected by TXT. The data presented are representative of three independent experiments with Mo-DCs generated from three different healthy donors. OK-432 induced a considerable amount of IL-12 p70 in one of three cases. In this case, IL-12 p70 was also reduced at concentrations as low as 10^{-9} M (data not shown).

Effect of TXT on imMo-DC-mediated allogenic T-cell response

To determine whether expression of antigen presenta-tion-related molecules on imMo-DCs affects antigen-presenting potential, the ability of imMo-DCs to stim-ulate allogenic T-cell proliferation was determined by MLR as described in "Materials and methods". TXT at concentrations greater than 10^{-7} M significantly de-creased [³H]-thymidine uptake, suggesting that TXT decreases the ability of imMo-DCs to stimulate allogenic T-cell proliferation (Fig. 7). The data presented are representative of three independent experiments with allogenic PBMCs and Mo-DCs generated from three different healthy donors.

Discussion

In the present study, we showed that TXT at different concentrations produced different effects on antigen presentation-related functions of Mo-DCs. The effect of TXT on Mo-DC motility is particularly notewor-thy.

ImDCs are capable of antigen capture [9]. How-ever, DCs must mature and be adequately activated to become effective APCs. DCs that are insufficiently mature may induce immune tolerance rather than immune responsiveness [3]. It is generally accepted that antigen presentation-related functions of Mo-DCs are closely similar to those of DCs. Since TXT of 10^{-7} M did not affect Mo-DC viability, phagocytosis, or expression of antigen presentation-related surface molecules (Figs. 1 and 5), it is unlikely that patients receiving TXT in the clinic would have impaired imDC or imMo-DC function. Nevertheless, we have to recognize the possibility that TXT at high doses may weaken antigen-presenting ability, because TXT at 10^{-7} M suppressed allogenic T-cell proliferation by imMo-DCs (Fig. 7).

We wish to emphasize that TXT even at concen-trations lower than 10^{-8} M impaired the motility of both imMo-DCs and mMo-DCs (Fig. 3). ImDCs re-spond to a large spectrum of chemokines through specific receptors. MIP-3α appears to be the most powerful chemokine guiding imDCs [8]. However, MIP-3α has no effect on imMo-DCs [3, 8]. In this

study, therefore, we chose MIP-1α as the chemokine for imMo-DCs [3]. Hotchkiss et al. [21] have reported that TXT at a very low concentration $(10^{-12}\ M)$ reduces the migratory ability of endothelial cells. Substoichiometric binding of taxanes suppresses microtubule dynamics [10]. These findings imply that drug-mediated effects on microtubule plasticity/ dynamics rather than on gross microtubule organization or expression are sufficient for inhibition of cell locomotion. Cell migration usually requires adhesion of cells to matrices such as integrins and fibronectin.

Podosomes are actin-rich adhesion structures found in monocyte-derived cells [12]. Although the roles of podosomes in cell spreading and migration and the mechanisms of their formation or dissolution are not yet clearly understood, a close relationship between microtubules and podosomes has been suggested [34]. For example, partial disassembly of microtubules leads to a more random pattern of podosome distribution [26]. Recently, it has been shown that microtubules are essential for podosome formation in human macrophages: freshly isolated monocytes undergoing adhesion fail to develop podosomes when treated with microtubule-depolymerizing drugs [26]. TXT at $10^{-8}\ M$ induced random podosome distribution in Mo-DCs and decreased their adhesive ability, even though TXT at this concentration only slightly impaired a radial microtubule array formation (Fig. 2). Moreover, our data suggest that TXT at concentrations as low as $10^{-9}\ M$ is able to alter microtubule dynamics and that a functional relationship exists between microtubules, podosomes, migration, and adhesion.

It is also noteworthy that TXT at $10^{-10}\ M$ reduced IL-12 p40 production from OK-432-stimulated imMo-DCs (Fig. 6). Although our previous data showed that phagocytic ability plays an important role in IL-12 production from OK-432-stimulated imMo-DCs, TXT at concentrations lower than $10^{-7}\ M$ did not affect phagocytosis of OK-432 by imMo-DCs (data not shown). We also note that TXT at $10^{-7}\ M$ did not affect IL-12 p40 production of imMo-DCs without OK-432 stimulation. These results underscore the complexity of OK-432-stimulated imMo-DC IL-12 production, which involves antigen capture, antigen processing, and finally IL-12 production.

The ability of TXT at very low concentrations to suppress the motility of DCs is important because only motile DCs are capable of inducing primary sensitization against specific antigens in naive T cells. When patients undergo chemotherapy with taxanes, we should pay more attention to their immunity. TXT-induced immunosuppression may increase the risk of infection in patients. Moreover, in the future, Mo-DCs are likely to be used in immunotherapy in combination with taxanes for treatment of cancer. The possibility that taxane treatment will decrease Mo-DC motility and consequently Mo-DC vaccine efficacy will have to be carefully considered.

References

1. Axel DI, Kunert W, Goggelmann C, Oberhoff M, Herdeg C, Kuttner A, Wild DH, Brehm BR, Riessen R, Koveker G, Karsch KR (1997) Paclitaxel inhibits arterial smooth muscle cell proliferation and migration in vitro and in vivo using local drug delivery. Circulation 96:636
2. Banchereau J, Steinman RM (1998) Dendritic cells and the control of immunity. Nature 392:245
3. Banchereau J, Briere F, Caux C, Davoust J, Lebecque S, Liu YJ, Pulendran B, Palucka K (2000) Immunobiology of dendritic cells. Annu Rev Immunol 18:767
4. Banchereau J, Palucka AK, Dhodapkar M, Burkeholder S, Taquet N, Rolland A, Taquet S, Coquery S, Wittkowski KM, Bhardwaj N, Pineiro L, Steinman R, Fay J (2001) Immune and clinical responses in patients with metastatic melanoma to CD34(+) progenitor-derived dendritic cell vaccine. Cancer Res 61:6451
5. Belotti D, Rieppi M, Nicoletti MI, Casazza AM, Fojo T, Taraboletti G, Giavazzi R (1996) Paclitaxel (Taxol) inhibits motility of paclitaxel-resistant human ovarian carcinoma cells. Clin Cancer Res 2:175
6. Bruno R, Vergniol JC, Montay G (1992) Clinical pharmacology of taxotere (RP 56976) given as 1–2 hr infusion every 2–3 weeks. Proc Am Assoc Cancer Res 32:261
7. Burns S, Hardy SJ, Buddle J, Yong KL, Jones GE, Thrasher AJ (2004) Maturation of DC is associated with changes in motile characteristics and adherence. Cell Motil Cytoskeleton 57:118
8. Caux C, Ait-Yahia S, Chemin K, de Bouteiller O, Dieu-Nosjean MC, Homey B, Massacrier C, Vanbervliet B, Zlotnik A, Vicari A (2000) Dendritic cell biology and regulation of dendritic cell trafficking by chemokines. Springer Semin Immunopathol 22:345
9. Cella M, Sallusto F, Lanzavecchia A (1997) Origin, maturation and antigen presenting function of dendritic cells. Curr Opin Immunol 9:10
10. Derry WB, Wilson L, Jordan MA (1995) Substoichiometric binding of taxol suppresses microtubule dynamics. Biochemistry 34:2203
11. Engleman EG, Fong L (2003) Induction of immunity to tumor-associated antigens following dendritic cell vaccination of cancer patients. Clin Immunol 106:10
12. Evans JG, Correia I, Krasavina O, Watson N, Matsudaira P (2003) Macrophage podosomes assemble at the leading lamella by growth and fragmentation. J Cell Biol 161:697
13. Fong L, Engleman EG (2000) Dendritic cells in cancer immunotherapy. Annu Rev Immunol 18:245
14. Gelmon K (1994) The taxoids: paclitaxel and docetaxel. Lancet 344:1267
15. Glasgow JE, Daniele RP (1994) Role of microtubules in random cell migration: stabilization of cell polarity. Cell Motil Cytoskeleton 27:88
16. Gluck S (2001) The worldwide perspective in the adjuvant treatment of primary lymph node positive breast cancer. Breast Cancer 8:321
17. Goodsell DS (2000) The molecular perspective: microtubules and the taxanes. Oncologist 5:345
18. Herrin VE, Thigpen JT (1999) Chemotherapy for ovarian cancer: current concepts. Semin Surg Oncol 17:181
19. Hortobagyi GN (1999) Recent progress in the clinical development of docetaxel (Taxotere). Semin Oncol 26(3 Suppl 9):32
20. Hortobagyi GN (2002) Integration of docetaxel into adjuvant breast cancer treatment regimens. Oncology (Huntingt) 16(6 Suppl 6):27
21. Hotchkiss KA, Ashton AW, Mahmood R, Russell RG, Sparano JA, Schwartz EL (2002) Inhibition of endothelial cell function in vitro and angiogenesis in vivo by docetaxel (Taxotere): association with impaired repositioning of the microtubule organizing center. Mol Cancer Ther 1:1191

22. Kellermann SA, Hudak S, Oldham ER, Liu YJ, McEvoy LM (1999) The CC chemokine receptor-7 ligands 6Ckine and macrophage inflammatory protein-3 beta are potent chemoattractants for in vitro- and in vivo-derived dendritic cells. J Immunol 162:3859

23. Kris MG, Tonato M (2002) New approaches in the treatment of non-small cell lung cancer: taxanes in the treatment of NSCLC: pathways to progress. Lung Cancer 38 [Suppl 4]:1

24. Kuroki H, Morisaki T, Matsumoto K, Onishi H, Baba E, Tanaka M, Katano M (2003) Streptococcal preparation OK-432: a new maturation factor of monocyte-derived dendritic cells for clinical use. Cancer Immunol Immunother 24:4443

25. Linder S, Aepfelbacher M (2003) Podosomes: adhesion hotspots of invasive cells. Trends Cell Biol 13:376

26. Linder S, Hufner K, Wintergerst U, Aepfelbacher M (2000) Microtubule-dependent formation of podosomal adhesion structures in primary human macrophages. J Cell Sci 113:4165

27. Luft T, Jefford M, Luetjens P, Toy T, Hochrein H, Masterman KA, Maliszewski C, Shortman K, Cebon J, Maraskovsky E (2002) Functionally distinct dendritic cell (DC) populations induced by physiologic stimuli: prostaglandin E(2) regulates the migratory capacity of specific DC subsets. Blood 100:1362

28. Morse MA, Lyerly HK (2000) Dendritic cell-based immunization for cancer therapy. Adv Exp Med Biol 465:335

29. Morse MA, Zhou LJ, Tedder TF, Lyerly HK, Smith C (1997) Generation of dendritic cells in vitro from peripheral blood mononuclear cells with granulocyte-macrophage-colony-stimulating factor, interleukin-4, and tumor necrosis factor-alpha for use in cancer immunotherapy. Ann Surg 226:6

30. Obasaju C, Hudes GR (2001) Paclitaxel and docetaxel in prostate cancer. Hematol Oncol Clin North Am 15:525

31. Onishi H, Morisaki T, Baba E, Kuga H, Kuroki H, Matsumoto K, Tanaka M, Katano M (2002) Dysfunctional and short-lived subsets in monocyte-derived dendritic cells from patients with advanced cancer. Clin Immunol 105:286

32. Roberts RL, Nath J, Friedman MM, Gallin JI (1982) Effects of taxol on human neutrophils. J Immunol 129:2134

33. Rodriguez OC, Schaefer AW, Mandato CA, Forscher P, Bement WM, Waterman-Storer CM (2003) Conserved microtubule-actin interactions in cell movement and morphogenesis. Nat Cell Biol 5:599

34. Shutt DC, Daniels KJ, Carolan EJ, Hill AC, Soll DR (2000) Changes in the motility, morphology, and F-actin architecture of human dendritic cells in an in vitro model of dendritic cell development. Cell Motil Cytoskeleton 46:200

35. Small JV, Geiger B, Kaverina I, Bershadsky A (2002) How do microtubules guide migrating cells? Nat Rev Mol Cell Biol 3:957

36. Swetman CA, Leverrier Y, Garg R, Gan CH, Ridley AJ, Katz DR, Chain BM (2002) Extension, retraction and contraction in the formation of a dendritic cell dendrite: distinct roles for Rho GTPases. Eur J Immunol 32:2074

37. Terzis AJ, Thorsen F, Heese O, Visted T, Bjerkvig R, Dahl O, Arnold H, Gundersen G (1997) Proliferation, migration and invasion of human glioma cells exposed to paclitaxel (Taxol) in vitro. Br J Cancer 75:1744

38. Trinchieri G (1995) Interleukin-12: a proinflammatory cytokine with immunoregulatory functions that bridges innate resistance and antigen-specific adaptive immunity. Annu Rev Immunol 13:251

39. Tsavaris N, Kosmas C, Vadiaka M, Kanelopoulos P, Boulamatsis D (2002) Immune changes in patients with advanced breast cancer undergoing chemotherapy with taxanes. Br J Cancer 87:21

40. Westerlund A, Hujanen E, Hoyhtya M, Puistola U, Turpeenniemi-Hujanen T (1997) Ovarian cancer cell invasion is inhibited by paclitaxel. Clin Exp Metastasis 15:318

41. Yu B, Kusmartsev S, Cheng F, Paolini M, Nefedova Y, Sotomayor E, Gabrilovich D (2003) Effective combination of chemotherapy and dendritic cell administration for the treatment of advanced-stage experimental breast cancer. Clin Cancer Res 9:285

42. Zhang H, Morisaki T, Nakahara C, Matsunaga H, Sato N, Nagumo F, Tadano J, Katano M (2003) PSK-mediated NF-kappaB inhibition augments docetaxel-induced apoptosis in human pancreatic cancer cells NOR-P1. Oncogene 22:2088

43. Zhou LJ, Tedder TF (1996) CD14+ blood monocytes can differentiate into functionally mature CD83+ dendritic cells. Proc Natl Acad Sci U S A 93:2588

44. Zlotnik A, Yoshie O (2000) Chemokines: a new classification system and their role in immunity. Immunity 12:127

Combination Therapy with Tumor Cell-pulsed Dendritic Cells and Activated Lymphocytes for Patients with Disseminated Carcinomas

MITSUO KATANO[1], TAKASHI MORISAKI[1], KENNICHIRO KOGA[1], MITSUNARI NAKAMURA[2],
HIDEYA ONISHI[1], KOTARO MATSUMOTO[1], AKIRA TASAKI[1], HIROSHI NAKASHIMA[1],
TAKASHI AKIYOSHI[1] and MASAFUMI NAKAMURA[1]

[1]Department of Cancer Therapy and Research, Graduate School of Medical Sciences,
Kyushu University, 3-1-1 Maidashi, Higashi-ku, Fukuoka 818-8582;
[2]Sada Hospital, Fukuoka 812-8582, Japan

Abstract. *This phase I study was performed to assess the safety and immune response of tumor cell-pulsed dendritic cell (DC) vaccine therapy against cancer patients with multiple metastases. DCs, generated from adherent cells of peripheral blood mononuclear cells (PBMCs) using interleukin-4 (IL-4) and granulocyte/monocyte colony-stimulating factor, were loaded with autologous necrotic whole tumor cells. Thereafter, the DCs were matured with culture supernatants of OK-432-stimulated PBMCs. Activated lymphocytes were also induced from non-adherent cells of PBMCs using OKT-3 and IL-2. Patients received a subcutaneous injection of DCs loaded with tumor cells every 2 weeks and received an intravenous injection of activated lymphocytes every 4 weeks. This combination therapy was named tumor-pulsed DC vaccine therapy. Tumor-pulsed DC vaccine therapy was continued as long as possible in 19 patients. No particular adverse reactions, except for low-grade fever, were found. The patients could be divided into two groups according to the survival time, i.e., 6 responders (long survival patients) and 13 non-responders (short survival patients). Based on the laboratory data of responders, eligibility criteria were determined. Using the eligibility criteria, a phase I/II study was recently performed with 15 patients. A delayed-type hypersensitivity reaction against tumor-pulsed DCs became positive in 13 of the 15 patients within 6 months after the therapy. This therapy was again safe, and no evidence of autoimmune disease was noted. The survival time of these 15 patients was significantly prolonged compared with that of the 13 non-responders of the phase I study (p<0.0001). This continuous tumor-pulsed DC vaccine therapy was well tolerated in patients with disseminated carcinomas.*

Although it has been shown that tumors possess antigenicity, which can induce specific immunity against tumors, immunotherapy targeting these antigenic molecules is successful only in limited cases (1). Recent advances in immunology have highlighted the importance of understanding the complex interactions between innate immunity and acquired immunity for the establishment of successful cancer immunotherapy. Among immune cells, the main players are dendritic cells (DCs) (2-4). Consequently, DC-based vaccine therapies with DCs loaded with various tumor-associated antigens (TAAs), such as tumor lysate (5), tumor-derived peptides (6), synthetic peptides (7), or tumor-derived RNA (8), are now under way. Synthetic peptides are very useful as antigen sources against known TAAs of target tumors. However, it is believed that the antigenicity of tumors is heterogeneous, and that some tumor cells do not contain the target TAAs (9, 10). Therefore, we used DCs loaded with whole tumor cells that contain both known and unknown TAAs (11). DC-based vaccine therapy is usually of 6-month duration (12, 13), however, in this clinical trial, the DC vaccine therapy was continued for as long as possible.

Materials and Methods

Patients. This phase I study included 19 inoperable cancer patients with multiple metastases, according to a protocol approved by the

Table I. *Patient characteristics and adverse events (phase I study).*

Patient no.	Age (yrs)/ Gender	Site of primary tumor	Site of metastases	Previous therapy	Adverse reaction
1	38/Male	Rectum	Lung, bone	Chemotherapy	Low-grade fever
2	49/Male	Bile-duct	Lung, Pl, LN	Chemotherapy	None
3	65/Female	Pancreas	Pt, Liver	Chemotherapy	None
4	46/Female	Stomach	Pt	Chemotherapy	Low-grade fever
5	72/Female	Pancreas	Liver, Pt, skin	Chemotherapy	None
6	72/Male	Large intestine	Liver, LN	None	Low-grade fever
7	56/Female	Gall bladder	Liver, Pt	Chemotherapy	Low-grade fever
8	49/Male	Gall bladder	Liver	None	None
9	73/Male	Gall bladder	Liver, Pt	Chemotherapy	Low-grade fever
10	41/Male	Stomach	Pt, LN	None	None
11	49/Female	Rectum	Pt, bone	Chemotherapy	Eosinophilia
12	49/Male	Stomach	Pt	None	Low-grade fever
13	45/Female	Rectum	Pt, bone	None	None
14	54/Female	Pancreas	LN	None	Low-grade fever
15	73/Male	Lung	Lung, skin, LN	Chemotherapy	None
16	66/Male	Stomach	Pt	None	Low-grade fever
17	68/Male	Lung	Lung, LN	Chemotherapy	None
18	54/Female	Ovary	Pl, Pt	Chemotherapy	None
19	65/Male	Rectum	Lung, Pt	None	None

Pl: pleural membrane, LN: lymph node, Pt: peritoneum.

Kyushu University Ethics Committee, Japan. Inclusion criteria were: histologically confirmed cancer, not amenable to cure by any standard therapy; performance status of 0, 1 or 2 on the ECOG scale; a minimum estimated life expectancy of 3 months; adequate hematological, hepatic and renal function; age>18 years; presence of obtainable tumor cells. The clinical details of the patients are summarized in Table I. Based on data of the phase I trial, a phase I/II trial was recently performed with 15 patients who satisfied at least 2 of the 4 following eligibility criteria: absolute lymphocyte count more than 1,000/µl, serum total protein level more than 6 g/dl, hemoglobin more than 10 g/dl, and a positive PPD skin test. The clinical details of the patients are summarized in Table II.

Study design. Each patient received a subcutaneous injection of 2-30x10⁶ mature DCs loaded with necrotic tumor cells into the left supraclavicular area, every 2 or 3 weeks. Intravenous injection of 1-5x10⁸ OKT3/IL-2-activated lymphocytes was combined with the above DC vaccine every 4 weeks. This combination therapy has been named tumor-pulsed DC vaccine therapy. In principle, this tumor-pulsed DC vaccine therapy was continued for as long as possible in the outpatient clinic.

Preparation of DCs loaded with necrotic tumor cells. Peripheral blood mononuclear cells (PBMCs) were collected by leukapheresis with a COBE spectrum apheresis system (GAMBRO BCT, Inc, CL, USA). PBMCs were suspended at a cell density of 4x10⁶ cells/ml in GMP-grade RPMI 1640 (Hy-Media; Nipro, Tokyo, Japan) supplemented with 1% human albumin, and 500 µl of the cell suspension were cultured for 4 h in 24-well culture plate. After non-adherent cells had been removed, the adherent cells were further cultured in Hy-Media containing 1% human albumin, 100 ng/ml of recombinant human granulocyte/monocyte colony-

Table II. *Patient characteristics and clinical outcome (phase I/II study).*

Patient no.	Age (yrs)/ Gender	Site of primary tumor	Site of metastases	Prognosis (Months)
1	40/Male	Rectum	Lung, bone	22, alive
2	49/Female	Rectum	Lung, Pt	14, dead
3	65/Male	Large intestine	Lung, Pt	16, alive
4	43/Male	Stomach	Bone, LN	11, dead
5	65/Female	Pancreas	Liver, Pt	10, dead
6	50/Female	Unknown	Liver, Pt	6, dead
7	55/Female	Pancreas	Pt, LN	15, alive
8	75/Male	Lung	Lung, Pl	7, alive
9	65/Male	Large intestine	Adrenal, LN	6, alive
10	45/Female	Stomach	Lung, Pt	5, dead
11	50/Male	Thymus	Lung, Pt	10, dead
12	55/Female	Stomach	Pt	6, alive
13	54/Female	Breast	Lung, Pt	6, alive
14	53/Female	Stomach	Pt, LN	6, alive
15	49/Female	Breast	Lung, Pt	4, alive

Pl: pleural membrane, LN: lymph node, Pt: peritoneum.

stimulating factor (GM-CSF; North China Pharmaceutical group Corporation-Gene Tech, China) and 50 ng/ml of recombinant human interleukin-4 (IL-4; Osteogenetics, Wuerburg, Germany) for 7 days. After 7 days, the cells were harvested as immature DCs.

Tumor specimens were obtained from the tumor mass or malignant effusions by surgical biopsy or parasenthesis, respectively. The tumor specimens were minced mechanically without chemical digestion. Thereafter, they were resuspended in 2
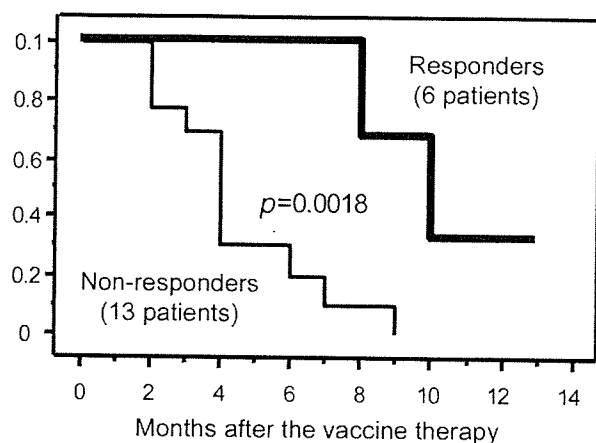
Figure 1. *Survival curves of the 19 patients enrolled in the phase 1 trial. According to the eligibility criteria described in Materials and Methods, 19 patients were divided into 6 suited patients (responders) and 13 unsuited patients (non-responders).*
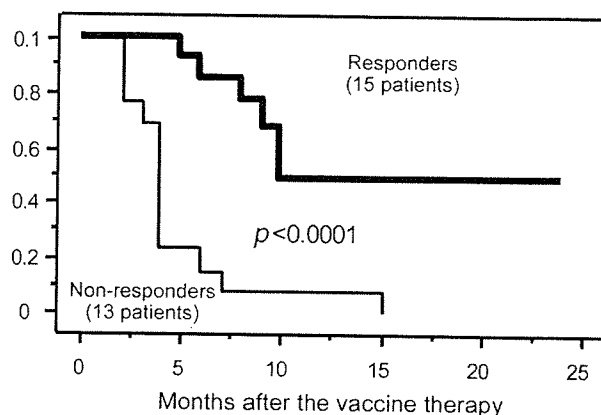

Figure 2. *Survival curves of the 15 patients who suited the eligibility criteria (phase I/II trial). The non-responders are the same as the non-responders of the phase 1 trial.*

ml of RPMI 1640 and lysed by 5 freeze and thaw cycles. The lysed cells (necrotic tumor cells) were used as a TAAs source.

Immature DCs were incubated with necrotic tumor cells overnight (DCs:tumor=5-10:1) and further cultured for 2 days in the medium containing 40% OK-432-induced PBMC culture supernatants to induce mature DCs (tumor cell-pulsed DCs). OK-432-induced PBMC culture supernatants were prepared by 1-day coculture of PBMCs (10^6/ml) of healthy volunteers and OK-432 (0.05 KE/ml) (14).

Preparation of activated lymphocytes. Non-adherent cells of patient's PBMCs were cultured for 2 weeks with Hy-medium containing 175 JRU/ml human recombinant IL-2 (Nipro) and immobilized monoclonal antibody to CD3 (10 μg/ml, OKT-3; Jansen-Kyowa, Tokyo, Japan).

Fluorescence-activating cell sorter (FACS) analysis. DCs ($1x10^5$) were suspended in 100 μl of diluted fluorescein-isothiocyanate or phycoerythrin-conjugated monoclonal antibodies (CD40, CD80, CD83, CD86, HLA-A, B and C, HLA-DR; Becton Dickinson, CA, USA) and assayed as described previously using a flow cytometer (FACS Caliber; Becton Dickinson) (14). The data were analyzed with CellQuest v3.2.1f1 (Becton Dickinson).

Measurement of serum tumor markers. Serum levels of tumor markers, including carcinoembryonic antigen (CEA), carbohydrate-antigen 19-9 (CA19-9), alpha fetoprotein (AFP) and DUPAN-2, were determined by enzymed-linked immunosorbent assay (ELISA).

Delayed-type hypersensitivity (DTH) reaction. One million tumor-pulsed DCs were injected intradermally into the forearm every 4 weeks. A positive DTH skin-test reaction was defined as >5 mm diameter erythema with induration 48 h after the DCs injection.

Enzyme-linked immunospot (ELISPOT) assay. Interferon-γ (IFN-γ)-producing PBMCs were assessed using an ELISPOT assay kit

according to the manufacturer's protocol (Diaclone Research, Besancon, France) (15). Briefly, PBMCs ($5x10^4$ cells), together with tumor cell-pulsed or non-pulsed DCs (10^4 cells), were plated on nitrocellulose 96-well plates (Millipore, Bedford, MA, USA) coated with anti-IFN-γ antibody and incubated for 15 h at 37°C. After removal of the cells, bound IFN-γ could be detected *via* a secondary biotinylated antibody. Streptavidine alkaline phosphatase binds to biotin and is detected *via* the BCIP/NBT substrate. The spots were counted with a stereomicroscope.

Clinical outcome. A partial response (PR) was defined as a decrease in all measurable tumor tissue of over 50% for at least 4 weeks without any new sign of disease. Stable disease (SD) was defined as a decrease in measurable tumor tissue of less than 50% and an increase of less than 25%. In this study, SD continuing for more than 6 months was named long SD.

Statistical analysis. The data were analyzed with a SAS statistical software package. Categorical variables were compared using Fisher's exact test. *P*-values less than 0.05 were considered statistically significant. The estimated probability of survival was demonstrated using the Kaplan-Meier method. The Mantel Cox log-rank test was used to compare curves between responders and non-responders.

Results

Phase I study. Nineteen patients, including 5 large intestinal cancer, 4 gastric cancer, 4 biliary tract cancer, 3 pancreatic cancer, 2 lung cancer and 1 ovarian cancer, were entered into this phase I trial. All of these patients were evaluated as progressive disease (PD) at the time of entry to the study (Table I). The patients received the tumor-pulsed DC vaccine therapy for as long as possible. No patient had to leave the study for safety reasons during this trial period of 1 year, because no severe adverse